Enumeration and Structural Classification of Clusters Derived from Parent Solids: Metal–Chalcogenide Clusters Composed of Edge-Sharing Tetrahedra

ARTICLE *in* JOURNAL OF THE AMERICAN CHEMICAL SOCIETY · NOVEMBER 1994

Impact Factor: 12.11 · DOI: 10.1021/ja00101a020

2 AUTHORS, INCLUDING:

R. H. Holm
Harvard University
339 PUBLICATIONS **17,528** CITATIONS

Enumeration and Structural Classification of Clusters Derived from Parent Solids: Metal–Chalcogenide Clusters Composed of Edge-Sharing Tetrahedra

Jeffrey R. Long[1] and R. H. Holm*

Contribution from the Department of Chemistry, Harvard University, Cambridge, Massachusetts 02138

Received April 15, 1994®

Abstract: A general method for the computer-assisted generation of polyhedra-based cluster structures is introduced. The cluster family of interest is delimited, and its definitive structural elements are employed in the design of an infinitely extended parent solid. For computational facility, this polyhedra-based solid is transformed into a parallel graph representation consisting of a simple lattice of points and lines. In connection with the structure–graph relationship, a descriptive notation detailing the local connectivity of constituent polyhedra is developed for use with both clusters and solids. Pieces of the lattice, corresponding to fragments of the parent solid, are generated by a straightforward recursive procedure. These fragments are converted into ligated clusters, and their structures are compiled in a database. Database structures are then subjected to four types of cluster rearrangement processes (folding, fusion, closure, and condensation) defined herein. Any relevant new structures which result are added to the database. The database is arranged by chemical formulae, and clusters of particular interest are sorted from it by whatever criteria are deemed appropriate. With the aid of electronic energy calculations, relative stabilities of structural isomers may then be evaluated, leading to some measure of predictive capability. The primary advantage of this approach lies in its ability to produce immediately accessible structures with tailored stereochemistries. The entire procedure is demonstrated for edge-sharing tetrahedra-based structures typical of the iron–sulfur/selenium cluster family. These structures, derived from a parent solid with the antifluorite structure, are enumerated for formulae containing eight or fewer tetrahedral metal centers. Attention is focused on clusters with chalcogenide bridging modalities of four or less, and containing one or fewer associated terminal ligands per metal atom. Relative energies of selected $[Fe_mS_qCl_l]^{n-}$ isomers with $m < 7$ are calculated via the extended Hückel method, and on the basis of these results, structures are proposed for some possible synthetic targets. Applications involving cluster synthesis, structural models employed during the crystallographic resolution of cluster-containing biomolecules, and elucidation of laser ablated cluster ions are briefly discussed.

Introduction

Recent work from this laboratory represents the first step in the structural systemization of metal–chalcogenide (M–Q) clusters containing four-coordinate metal sites.[2] In this analysis, matrix methods are employed in enumerating Q atom bridging modalites and generating connectivity patterns for clusters of a specified stoichiometry, $M_mQ_qL_l$, where L is a terminal ligand. The results provide a previously unavailable assessment of the scope of the structural chemistry of these clusters. Difficulties arise, however, with attempts at translating the connectivities into meaningful structures. Due to the lack of a suitable algorithm for idealizing the metrics of a cluster, the task becomes a formidable heuristic endeavor, especially for higher nuclearities. Moreover, the majority of the structures thus obtained must be rejected as stereochemically implausible or even impossible. The problem is inherent in connectivity matrices. Given that A is connected to B and B is connected to C, is it possible to connect A and C? From the standpoint of the matrix, it surely is, but for slightly more rigid bodies (such as atoms in molecules) it is not necessarily possible.

In addressing these problems we have arrived at a new, widely applicable approach to cluster generation. One fairly obvious way of overcoming the stereochemical problem is to begin by imposing a *specific* stereochemistry on some or all of the atoms. For example, four-coordinate M atoms might be restricted to ideal tetrahedral coordination. In so doing, some structural versatility is lost, but the loss is compensated by confidence in the feasibility of the resulting structures. Still, there remains the issue of accessing these structures. This problem may be solved by utilizing a carefully chosen infinite parent solid as a source of clusters in the form of solid fragments. Thus, the cluster structures are implicit in the parent solid. Additional ease in the computer-aided generation of new structures may then be attained by invoking some of the formalism of graph theory.

This new approach inevitably leads to the recognition of an underlying structural relationship between molecular clusters and extended solids. Recently, the cluster–solid relationship has been emphasized through nanophase research, in which nanometer-scale crystallites are found to exhibit a behavior intermediate to that of molecules and solids.[3] These nanoclusters provide an indisputable link between clusters and solids, while further demonstrating the practicality of viewing certain clusters as ligand-stabilized pieces of an extended solid, an idea which is by no means new. For example, at an early stage in molecular cluster chemistry it was recognized that metal carbonyl clusters could "be considered as finite parts of close-packed metallic structures".[4] Despite the vast number of new clusters synthesized as a result of this and similar ideas, relatively few of them have been explicitly

® Abstract published in *Advance ACS Abstracts,* September 15, 1994.

(1) Office of Naval Research Predoctoral Fellow, 1991–1994.

(2) You, J.-F.; Holm, R. H. *Inorg. Chem.* **1992**, *31*, 2166.

(3) (a) Steigerwald, M. L.; Brus, L. E. *Annu. Rev. Mater. Sci.* **1989**, *19*, 471. (b) Heinglein, A. *Chem. Rev.* **1989**, *89*, 1861. (c) Stucky, G. D.; Mac Dougall, J. E. *Science* **1990**, *247*, 669. (d) Wang, Y.; Herron, N. *J. Phys. Chem.* **1991**, *95*, 525. (e) Schmid, G. *Chem. Rev.* **1992**, *92*, 1709. (f) Weller, H. *Angew. Chem., Int. Ed. Engl.* **1993**, *32*, 41.

(4) Chini, P. *Inorg. Chim. Acta Rev.* **1968**, *2*, 31.

(5) It should be noted that a number of nonmolecular solids are built up of discrete clusters (often with molecular analogues) linked via bridging atoms in one, two, and three dimensions.[6] The clusters contained in these solids may also be described as pieces of other, more condensed solids in which finite clusters are not distinguishable. Subsequently, they would not generally be considered as parent solids given the present context.

0002-7863/94/1516-9987$04.50/0

Table 1. Examples of Structurally Proven Clusters Containing Cores[a] Described as Solid Fragments

cluster[b]	solid	ref
$V_2(S_2)_2(S_2CN^iBu_2)_4$	VS_4	7
$[Fe_3S_4(SPh)_4]^{3-}$	$KFeS_2$	8
$[V_4O_8(NO_3)(tca)_4]^{2-}$	V_2O_5	9
$Ta_5N_5(^tBuCH_2)_{10}$	TaN (cubic)	10
$Pd_6Te_6(PEt_3)_8$	PdTe	11
$Si_7O_9(OH)_3Cy_7$	SiO_2 (β-cristobalite)	12
$[Ni_8S(S^tBu)_9]^{1-}$	NiS (hexagonal)	13
$Al_{10}(OH)_{16}(OSiEt_3)_{14}$	AlO(OH) (boehmite)	14
$[M_{10}S_4(SPh)_{16}]^{4-}$ (M = Zn, Cd)	α-MS	15
$[Y_2Cu_8O_2(OPy)_{12}Cl_2]^{4+}$	$YBa_2Cu_3O_{7-x}$	16
$[AlSi_{15}O_{25}Cy_{14}]^{1-}$	zeolite Linde A	17
$[Fe_{19}O_6(OH)_{14}(heidi)_{10}(H_2O)_{12}]^{1+}$	FeO(OH) (goethite)	18
$Li_{20}(1\text{-}C_7H_{10}N)_{10}(Et_2O)_6$	Li_2NH	19
$Cd_{32}S_{14}(SPh)_{36}$	α-CdS	20

[a] In many cases, the cluster contains a polyatomic ligand, one atom of which is considered part of the core. [b] tca = thiophene-2-carboxylate; Cy = cyclohexyl; H_3heidi = $N(CH_2COOH)_2(CH_2CH_2OH)$.

described in terms of their relation to a parent solid.[5] Table 1 contains a selection of clusters that have been recognized by the referenced authors as deriving from known extended solids without undergoing any major structural rearrangement.[7-20] In a few instances, one further step has been taken, and clusters have been subjected to varying degrees of structural reorganization prior to comparison with a parent solid.[9b,21] Such reorganizational processes will be discussed in more detail below.

Here we present a general method for deriving the structures of all possible finite clusters contained in a parent solid. The technique is demonstrated by application to clusters built up from edge-sharing tetrahedra of which iron–sulfur/selenium clusters comprise the most highly developed and best-known group.

Graph Theory

Many of the various applications of graph theory devised over the past century and a half pertain to chemistry.[22] In fact, chemistry has had a marked influence in the development of much of the theory, which has become an integral branch of combinatorial analysis. Enumeration problems for isomers of alkanes and alcohols prompted much of the initial work in the field, culminating in Pólya's theorem which enables a direct solution to these and similar counting problems. At roughly the same time, the use of adjacency matrices in the representation of molecules resulted in the formulation of Hückel theory. Manifold applications followed, including several concerning inorganic clusters[23] and solid state chemistry.[24] Here we demonstrate an application that effectively bridges these two areas. The formalism of graph theory provides a remarkably suited framework within which the problem of cluster enumeration is readily approached. We next introduce some basic concepts and definitions relevant to the problem. The definitions furnished here favor simplicity over rigor. More rigorous definitions, as well as many aspects of the theory not mentioned, may be found in some standard introductory texts.[25]

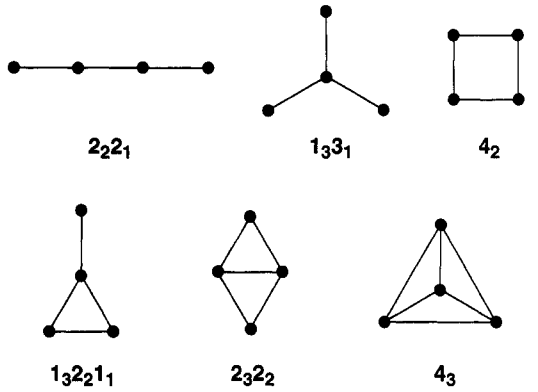

Figure 1. Diagrams and descriptive notation for all of the different animals containing four points.

A *graph* is a collection of points, some, all, or none of which are connected by lines. The actual position of the points is of no consequence, rather it is their connectivity pattern that characterizes a graph. Thus the two drawings (or *diagrams*) in **1** depict identical graphs. A *walk* of a graph is a sequence of its points interspersed with connecting lines. A walk which begins and ends with the same point is a *cycle*, provided all other points in the walk are distinct. For example, the triangle in the lefthand diagram of **1** is one of the three cycles contained in this graph. The same cycle may be obtained from the right-hand diagram by traversing its perimeter. If all the points in a walk are distinct, it is called a *path*. A graph is *connected* if each pair of its points is joined by a path. The graph in **1** is not connected, since it contains an *isolated* point that does not have a path to any other point. A connected graph is called an *animal*, and a connected graph with no cycles is called a *tree*. Note that a tree is also an animal, but animals are not necessarily trees. All of the different possible animals with four points are diagrammed in Figure 1. The two upper left animals, containing no cycles, are also trees.

1

It is often desirable to present a graph in a more succinct form than achieved with a diagram. A form widely used for computational purposes is the adjacency or connectivity matrix, in which the entry in row i and column j is 1 if points i and j are

(6) Lee, S. C.; Holm, R. H. *Angew. Chem., Int. Ed. Engl.* **1990**, *29*, 840.
(7) Halbert, T. R.; Hutchings, L. L.; Rhodes, R.; Stiefel, E. I. *J. Am. Chem. Soc.* **1986**, *108*, 6437.
(8) Hagen, K. S.; Watson, A. D.; Holm, R. H. *J. Am. Chem. Soc.* **1983**, *105*, 3905.
(9) (a) Heinrich, D. D.; Folting, K.; Streib, W. E.; Huffman, J. C.; Christou, G. *J. Chem. Soc., Chem. Commun.* **1989**, 1411. (b) Klemperer, W. G.; Marquart, T. A.; Yaghi, O. M. *Angew. Chem., Int. Ed. Engl.* **1992**, *31*, 49.
(10) Banaszak Holl, M. M.; Wolczanski, P. T.; Van Duyne, G. D. *J. Am. Chem. Soc.* **1990**, *112*, 7989.
(11) Brennan, J. G.; Siegrist, T.; Stuczynski, S. M.; Steigerwald, M. L. *J. Am. Chem. Soc.* **1990**, *112*, 9233.
(12) Feher, F. J.; Newman, D. A.; Walzer, J. F. *J. Am. Chem. Soc.* **1989**, *111*, 1741.
(13) Krüger, T.; Krebs, B.; Henkel, G. *Angew. Chem., Int. Ed. Engl.* **1989**, *28*, 61.
(14) Apblett, A. W.; Warren, A. C.; Barron, A. R. *Chem. Mater.* **1992**, *4*, 167.
(15) Dance, I. G.; Choy, A.; Scudder, M. L. *J. Am. Chem. Soc.* **1984**, *106*, 6285.
(16) Wang, S.; Pang, Z.; Wagner, M. J. *Inorg. Chem.* **1992**, *31*, 5381.
(17) Feher, F. J.; Weller, K. J. *Organometallics* **1990**, *9*, 2638.
(18) Heath, S. L.; Powell, A. K. *Angew. Chem., Int. Ed. Engl.* **1992**, *31*, 191.
(19) Armstrong, D. R.; Barr, D.; Clegg, W.; Drake, S. R.; Singer, R. J.; Snaith, R.; Stalke, D.; Wright, D. S. *Angew. Chem., Int. Ed. Engl.* **1991**, *30*, 1707.
(20) Herron, N.; Calabrese, J. C.; Farneth, W. E.; Wang, Y. *Science* **1993**, *259*, 1426.
(21) (a) Brennan, J. G.; Siegrist, T.; Stuczynski, S. M.; Steigerwald, M. L. *J. Am. Chem. Soc.* **1989**, *111*, 9240. (b) Steigerwald, M. L.; Siegrist, T.; Stuczynski, S. M. *Inorg. Chem.* **1991**, *30*, 2256, 4940. (c) Nomikou, Z.; Schubert, B.; Hoffmann, R.; Steigerwald, M. L. *Inorg. Chem.* **1992**, *31*, 2201.
(22) (a) *Chemical Applications of Graph Theory*; Balaban, A. T., Ed.; Academic Press: London, 1976. (b) Trinajstic, N. *Chemical Graph Theory*; CRC Press: Boca Raton, FL, 1983. (c) *Graph Theory and Topology in Chemistry*; King, R. B., Rouvray, D., Eds.; Elsevier: Amsterdam, 1987.
(23) King, R. B. *Applications of Graph Theory and Topology in Inorganic Cluster and Coordination Chemistry*; CRC Press: Boca Raton, FL, 1993, and references therein.
(24) McLarnan, T. J.; Moore, P. B. In *Structure and Bonding in Crystals II*; O'Keefe, M., Navrotsky, A., Eds.; Academic Press: New York, 1981; Chapter 21, and references therein.
(25) (a) Harary, F. *Graph Theory*; Addison-Wesley: Reading, MA, 1969. (b) Bollobás, B. *Graph Theory*; Springer-Verlag: New York, 1979.

joined by a line and 0 otherwise. Despite the ease of their mathematical manipulation, matrices are visually much less informative (and even more cumbersome) than pictures. A more concise notation for use in classifying and distinguishing graphs may be developed from one of their fundamental properties. The *degree* of a point is the number of lines incident with it. The number of points, m, in a graph can be partitioned by degree to yield a compact descriptor that captures much of its essence:

$$n_{m-1}...n_2n_1n_0 \qquad (1)$$

Here n_i is the number of points with degree i. As demonstrated for the graphs in Figure 1, only nonzero n are reported, and the subscripts are retained. The descriptor alone supplies a surprising amount of information about the graph. For instance, since every line is incident with two points, the number of lines λ in a graph is simply

$$\lambda = [(m-1)n_{m-1} + ... + 2n_2 + 1n_1]/2 \qquad (2)$$

a result first obtained by Euler. With this information and a little thought, a graph diagram may be constructed from its descriptor. Alternatively, for graphs with $m < 7$, an appropriate diagram may be selected from a compilation of diagrams sorted by m and λ.[25a] Unfortunately, descriptors are not always unique, and occasionally more than one graph is derived. For example, exactly two graphs (one of which is diagrammed in **1**) have the descriptor $2_33_21_0$. The notation described here for graphs is easily adapted for use with polyhedra-based clusters and solids, leading to the polyhedra connectivity partioning (PCP) notation delineated in the Appendix and employed throughout the remainder of this work.

Clearly many parallels could be drawn between graphs and clusters. For our purposes we shall represent clusters as graphs in which points correspond to polyhedra and lines designate shared vertices, edges, or faces. As the term implies, cluster graphs are connected, and therefore, we need only concern ourselves with trees and animals. The problem of idealizing metrics for cluster structure carries over to graph diagrams, as is evident from the two very different diagrams in **1**. In a number of applications, it has proved useful to confine trees and animals to a lattice.[26] The resulting *lattice trees* and *lattice animals* differ in that their points have fixed relative positions, eliminating any structural ambiguity. Great care must be taken in specifying the type of lattice from which these species derive. The number of lattice animals with m points, for instance, is not the same for square and rectangular lattices. Unless otherwise specified, future use of the terms tree and animal will refer to those species deriving from the *simple cubic* lattice. The idea of restricting animals to a lattice should be viewed as directly analogous to the notion of restricting clusters to a parent solid.

General Approach

The present approach for generating a structurally exhaustive cluster database consists of eight steps, as outlined in Figure 2. (1) The original cluster family is delimited, and a parent solid is constructed from its definitive structural elements. (2) The parent solid is transformed into a simplified lattice of points and lines to facilitate computation. (3) Lattice animals corresponding to fragments of the parent solid are generated by a straightforward recursive procedure. (4) These animals are then converted to solid fragment structures. (5) Fragments are translated into ligated clusters, and their structures are entered in the cluster database. (6) All database clusters are subjected to a variety of structural rearrangements defined herein. Any new clusters which result are entered in the database. (7) Clusters of particular interest are sorted from the database by whatever criteria are deemed appropriate. (8) Electronic structure calculations at the desired level of sophistication are employed in determining the relative stabilities of structural isomers, leading to some measure of predictive capability. The details involved in putting this general method into practice are elaborated below, while the entire process is demonstrated for the iron–chalcogenide cluster family.

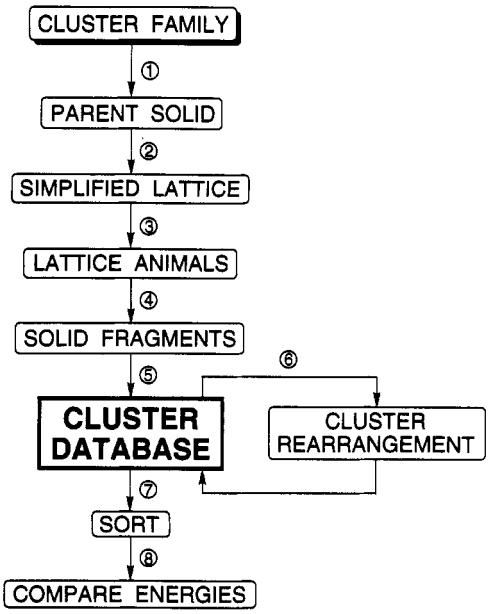

Figure 2. Flow chart outlining the general approach for cluster generation. Numbered steps are explained in the text.

The Parent Solid

The most vital step in this method for generating clusters is the initial selection of an appropriate parent solid. A poorly chosen solid may result in exclusion of reasonable structures and/or inclusion of unreasonable ones, invalidating attempts at structure enumeration and prediction. In this section, the process of choosing or creating a parent solid is described, largely by means of demonstration on our prototypic iron–chalcogenide system.

The family to be modeled by the solid must first be restricted to a well-defined set of clusters exhibiting those structural features deemed essential. Previous analyses have pointed out some characteristics common to most iron–chalcogenide clusters: roughly tetrahedral Fe sites, Fe–Q and Fe–L bonding but no strong Fe–Fe bonds, Q atoms with bridging multiplicities of two, three, or four, and cluster cores consisting largely or exclusively of edge- and/or vertex-sharing Fe_2Q_2 rhombs.[2,27] The lower nuclearity structures with these attributes are depicted in Figure 3 and include, *inter alia*, linear oligomer (**2**–**4**), cuboidal (**5**, **6**), cubane (**7**), prismane (**10**), and basket (**11**) clusters. Specific examples of each structural type are given in Table 2, along with some higher nuclearity compounds.[27b-56] A somewhat more pervasive structural theme is revealed in a list of the accompanying PCP descriptors: each cluster is composed primarily of edge-sharing metal-centered tetrahedra (hence the reduced PCP notation in which only the edge-sharing partition is reported). In general, preparing such a list provides an efficient means of

(26) Temperley, H. N. V. *Graph Theory and Applications*; Ellis Horwood Limited: Chichester, England, 1981; pp 49–70.

(27) (a) Reynolds, M. S.; Holm, R. H. *Inorg. Chem.* **1988**, *27*, 4494. (b) You, J.-F.; Snyder, B. S.; Papaefthymiou, G. C.; Holm, R. H. *J. Am. Chem. Soc.* **1990**, *112*, 1067. (c) You, J.-F.; Papaefthymiou, G. C.; Holm, R. H. *J. Am. Chem. Soc.* **1992**, *114*, 2697.

(28) Berg, J. M.; Holm, R. H. In *Iron–Sulfur Proteins*; Spiro, T. G., Ed.; Wiley-Interscience: New York, 1982; Chapter 1.

(29) Yu, S.-B.; Papaefthymiou, G. C.; Holm, R. H. *Inorg. Chem.* **1991**, *30*, 3476 and references therein.

(30) Bronger, W.; Ruschewitz, U.; Müller, P. *J. Alloys Comp.* **1992**, *187*, 95.

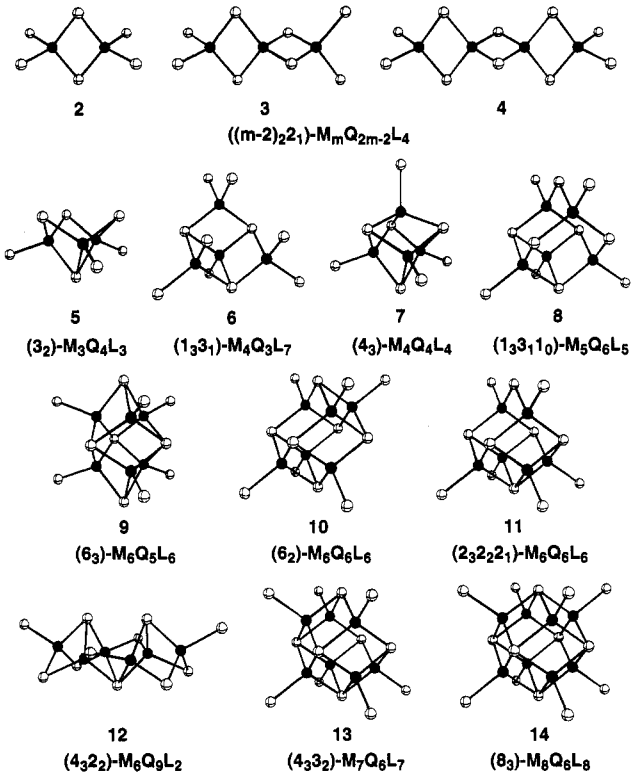

Figure 3. Idealized structures and reduced PCP notation for $M_mQ_qL_l$ clusters **2–14** with nuclearity m ranging from 2 to 8; examples are given in Table 2. Black spheres represent M. White spheres with multiple and single bonds represent Q and L, respectively.

structurally classifying the members in any given set of clusters. This classification often leads to the unavoidable exclusion of one or more apparent members. For example, the clusters SPy_2-(6_4)-$[Fe_6S_8(PEt_3)_6]^{2+,1+}$ are excluded from our Fe–Q family on the grounds that they do not contain tetrahedral iron sites.[57] Once the defining criteria have been established, the family can be expanded to incorporate any clusters or solids from other elemental systems that fulfill these structural requirements. Table 2 includes a number of non-iron transition metal–chalcogenide structures that are composed solely of edge-sharing tetrahedra and may consequently be adopted by the Fe–Q family.

Construction of a parent solid then proceeds through propagation of the polyhedra via appropriate vertex-sharing connections. For example, edge-sharing tetrahedra may be extended in one (**15**), two (**16**), and three (**17**) dimensions, as shown in Figures 4 and 5. The "infinite" chains, sheets, and networks that result are simply very large clusters, and provided they conform to the defining criteria, any known examples of these extended structures should be included in the cluster family. Fictitious or not, the solid of maximal dimension generally provides the most structural versatility, and is therefore the most suitable as a parent solid. Thus, although an Fe_2Q framework is unknown, we choose **17** for our Fe–Q parent. This is the *antifluorite* structure, and its aptitude as a parent for the Fe–Q family is made evident by cluster **14** which displays all of its unit cell contents. We now pose the certifying question: Does the cubic stereochemistry of the Q atoms in this structure form a reasonable model for the Q bridges found in other members of the cluster family? A re-examination of Figure 3 reveals that, with the exception of the μ_3-Q atom of the type found in **5** (the significance of which will be discussed below), all bridging Q situations are pieces of the $M_8(\mu_8\text{-}Q)$ cube. The existence of precisely this cubic arrangement in the cluster $Cu_8S(S_2P(OC_2H_5)_2)_6$[58] lends still further credibility to our parent solid.

In hindsight, the antifluorite structure seems a rather obvious choice as a parent for the iron–chalcogenide family. There are, however, a number of errors that might easily be made in selecting a parent solid for slightly more complex systems. The importance of maximizing the dimension of the solid cannot be overemphasized. Several iodoantimonate clusters have been described as pieces of the two-dimensional CdI_2 structure.[59] There exist three other known iodoantimonates[59b,60] that cannot be described as such, but which are recognizable fragments of the three-dimensional rock salt structure. The CdI_2 sheets are in fact slices of the rock salt structure, and the latter may be obtained from

(31) Hagen, K. S.; Watson, A. D.; Holm, R. H. *J. Am. Chem. Soc.* **1983**, *105*, 3905.
(32) Al-Ahmad, S. A.; Kampf, J. W.; Dunham, R. W.; Coucouvanis, D. *Inorg. Chem.* **1991**, *30*, 1163.
(33) (a) Bronger, W. *Naturwissenschaften* **1966**, *53*, 525; *Z. Anorg. Allg. Chem.* **1968**, *359*, 225; *Angew. Chem., Int. Ed. Engl.* **1981**, *20*, 52. (b) Boller, H.; Blaha, H. *Monatsh. Chem.* **1983**, *114*, 145.
(34) Bensch, W.; Stauber-Reichmuth, G.; Reller, A.; Oswald, H. R. *Rev. Chim. Miner.* **1987**, *24*, 503.
(35) (a) Robbins, A. H.; Stout, C. D. *Proc. Natl. Acad. Sci. U.S.A.* **1989**, *86*, 3639; *Proteins* **1989**, *5*, 289. (b) Stout, C. D. *J. Mol. Biol.* **1989**, *205*, 545. (c) Kissinger, C. R.; Adman, E. T.; Sieker, L. C.; Jensen, L. H. *J. Am. Chem. Soc.* **1988**, *110*, 8721. (d) Kissinger, C. R.; Sieker, L. C.; Adman, E. T.; Jensen, L. H. *J. Mol. Biol.* **1991**, *219*, 693.
(36) Hong, H. Y.; Steinfink, H. *J. Solid State Chem.* **1972**, *5*, 93.
(37) (a) Chu, C. T.-W.; Dahl, L. F. *Inorg. Chem.* **1977**, *16*, 3245. (b) Glidewell, C.; Lambert, R. J.; Harman, M. E.; Hursthouse, M. B. *J. Chem. Soc., Dalton Trans.* **1990**, 2685.
(38) Scott, M. J.; Holm, R. H. *Angew. Chem., Int. Ed. Engl.* **1993**, *32*, 564.
(39) (a) Carney, M. J.; Papaefthymiou, G. C.; Spartalian, K.; Frankel, R. B.; Holm, R. H. *J. Am. Chem. Soc.* **1988**, *110*, 6084 and references therein. (b) Carney, M. J.; Papaefthymiou, G. C.; Frankel, R. B.; Holm, R. H. *Inorg. Chem.* **1989**, *28*, 1497 and references therein. (c) O'Sullivan, T.; Millar, M. M. *J. Am. Chem. Soc.* **1985**, *107*, 4096. (d) Simon, W.; Wilk, A.; Krebs, B.; Henkel, G. *Angew. Chem., Int. Ed. Engl.* **1987**, *26*, 1009. (e) Barbaro, P.; Bencini, A.; Bertini, I.; Briganti, F.; Midollini, S. *J. Am. Chem. Soc.* **1990**, *112*, 7238.
(40) Bronger, W.; Kimpel, M.; Schmitz, D. *Angew. Chem., Int. Ed. Engl.* **1982**, *21*, 544.
(41) (a) Lei, X.-J.; Huang, Z.-Y.; Hong, M.-C.; Liu, Q.-T.; Liu, H.-Q. *Jiegou Huaxue* **1990**, *9*, 53. (b) Huang, Z.-Y.; Lei, X.-J.; Kang, B.-S.; Liu, J.-N.; Liu, Q.-T.; Hong, M.-C.; Liu, H.-Q. *Inorg. Chim. Acta* **1990**, *169*, 25.
(42) Manoli, J. M.; Potvin, C.; Secheresse; F.; Marzak, S. *J. Chem. Soc., Chem. Commun.* **1986**, 1557.
(43) (a) Nordlander, E.; Lee, S. C.; Cen, W.; Wu, Z. Y.; Natoli, C. R.; Di Cicco, A.; Filipponi, A.; Hedman, B.; Hodgson, K. O.; Holm, R. H. *J. Am. Chem. Soc.* **1993**, *115*, 5549. (b) Cen, W.; MacDonnell, F. M.; Scott, M. J.; Holm, R. H. *Inorg. Chem.*, in press.
(44) Fenske, D.; Ohmer, J. *Angew. Chem., Int. Ed. Engl.* **1987**, *26*, 148.
(45) (a) Coucouvanis, D.; Kanatzidis, M. G.; Dunham, W. R.; Hagen, W. R. *J. Am. Chem. Soc.* **1984**, *106*, 7998. (b) Kanatzidis, M. G.; Hagen, W. R.; Dunham, W. R.; Lester, R. K.; Coucouvanis, D. *J. Am. Chem. Soc.* **1985**, *107*, 953. (c) Kanatzidis, M.; Salifoglou, A.; Coucouvanis, D. *Inorg. Chem.* **1986**, *25*, 2460.
(46) (a) Snyder, B. S.; Reynolds, M. R.; Noda, I.; Holm, R. H. *Inorg. Chem.* **1988**, *27*, 595. (b) Snyder, B. S.; Holm, R. H. *Inorg. Chem.* **1988**, *27*, 2339. (c) Snyder, B. S.; Holm, R. H. *Inorg. Chem.* **1990**, *29*, 274.
(47) (a) Christou, G.; Sabat, M.; Ibers, J. A.; Holm, R. H. *Inorg. Chem.* **1982**, *21*, 3518. (b) Strasdeit, H.; Krebs, B.; Henkel, G. *Inorg. Chem.* **1984**, *23*, 1816; *Z. Naturforsch.* **1987**, *42B*, 565.
(48) Noda, I.; Snyder, B. S.; Holm, R. H. *Inorg. Chem.* **1986**, *25*, 3851.
(49) (a) Pohl, S.; Saak, W. *Angew. Chem., Int. Ed. Engl.* **1984**, *23*, 907. (b) Saak, W.; Pohl, S. *Angew. Chem., Int. Ed. Engl.* **1991**, *30*, 881. (c) Pohl, S.; Opitz, U. *Angew. Chem., Int. Ed. Engl.* **1993**, *32*, 863.
(50) Christou, G.; Hagen, K. S.; Bashkin, J. K.; Holm, R. H. *Inorg. Chem.* **1985**, *24*, 1010.
(51) Li, J.; Xin, X.; Zhou, Z.; Yu, K. *J. Chem. Soc., Chem. Commun.* **1991**, 249.
(52) You, J.-F.; Holm, R. H. *Inorg. Chem.* **1991**, *30*, 1431.
(53) Pruss, E. A.; Snyder, B. S.; Stacy, A. M. *Angew. Chem., Int. Ed. Engl.* **1993**, *32*, 256.
(54) Savelsberg, G.; Schäfer, H. *Z. Naturforsch.* **1978**, *33B*, 370, 711.
(55) (a) Müller, A.; Sievert, W. *Z. Anorg. Allg. Chem.* **1974**, *406*, 80. (b) Riedel, E.; Paterno, W.; Erb, W. *Z. Anorg. Allg. Chem.* **1977**, *437*, 127.
(56) Oliveria, M.; McMullan, R. K.; Wuensch, B. J. *Solid State Ionics* **1988**, *28*, 1332.
(57) (a) Agresti, A.; Bacci, M.; Cecconi, F.; Ghilardi, C. A.; Midollini, S. *Inorg. Chem.* **1985**, *24*, 689. (b) Cecconi, F.; Ghilardi, C. A.; Midollini, S.; Orlandini, A.; Zanello, P. *J. Chem. Soc., Dalton Trans.* **1987**, 831.
(58) Huang, Z.-X.; Lu, S.-F.; Huang, J.-Q.; Wu, D.-M.; Huang, J.-L. *Jiegou Huaxue* **1991**, *10*, 213.
(59) (a) Pohl, S.; Saak, W.; Haase, D. *Z. Naturforsch.* **1987**, *B42*, 1493. (b) Pohl, S.; Lotz, R.; Saak, W.; Haase, D. *Angew. Chem., Int. Ed. Engl.* **1989**, *28*, 344.
(60) (a) von Seyerl, J.; Scheidsteger, O.; Berke, H.; Huttner, G. *J. Organomet. Chem.* **1986**, *311*, 85. (b) Pohl, S.; Haase, D.; Lotz, R.; Saak, W. *Z. Naturforsch.* **1988**, *B43*, 1033.

Table 2. The Family of Structurally Established Transition Metal–Chalcogenide Compounds ($M_mQ_qL_l$) Composed Primarily of Edge-Sharing MX_4 (X = Q, L) Tetrahedra

formula	PCP[a]	examples[b]	ref
$M_mQ_{2m-2}L_4$	$T_2((\mathbf{m-2})_2\mathbf{2_1})$		
m = 2 (**2**)	$T_2(\mathbf{2_1})$	$[Fe_2Q_2L_4]^{2-}$; $[Fe_2Q_6]^{6-}$	28, 29; 30
m = 3 (**3**)	$T_2(\mathbf{1_22_1})$	$[Fe_3Q_4L_4]^{3-}$	29, 31
m = 4 (**4**)	$T_2(\mathbf{2_22_1})$	$[Fe_4Q_6L_4]^{4-}$	32
m = ∞ (**15**)	$T_2(\mathbf{1_2})$	$^1_\infty[FeQ_2]^{1-}$; $^1_\infty[MoCuS_4]^{1-}$	33; 34
$M_3Q_4L_3$ (**5**)	$T_2(\mathbf{3_2})$	$[Fe_3S_4(SR)_3]^{2-}$; $[Fe_3Se_7]^{6-}$	35; 36
$M_4Q_3L_7$ (**6**)	$T_2(\mathbf{1_33_1})T_1(3_2)$	$[Fe_4S_3(NO)_7]^{1-}$; $Fe_4S_3(NO)_4(PPh_3)_3$	37; 38
$M_4Q_4L_4$ (**7**)	$T_2(\mathbf{4_3})$	$[Fe_4Q_4L_4]^{1-,2-,3-}$;[c] $[Fe_4Te_8]^{7-}$	28, 29, 39; 40
$M_4Q_4L_6$ (**22**)	$T_2(\mathbf{1_33_1})T_1(1_22_1)$	$[MCu_3S_4(S_2CNEt_2)_3]^{2-}$ [d]	41
$M_5Q_4L_8$	$T_2(\mathbf{1_44_1})T_1(4_2)$	$^3_\infty[WCu_4S_4(NCS)_{8/2}]^{2-}$	42
$M_5Q_6L_5$ (**8**)	$T_2(\mathbf{1_33_1})T_1(4_3)$	$MFe_4S_6(PEt_3)_4Cl$[e]	43
$M_6Q_5L_6$ (**9**)	$T_2(\mathbf{6_3})T_1(6_2)$	$Ni_6Se_5(PPh_3)_6$	44
$M_6Q_6L_6$ (**10**)	$T_2(\mathbf{6_2})T_1(6_2)$	$[Fe_6S_6L_6]^{2-,3-}$	45
$M_6Q_6L_6$ (**11**)	$T_2(\mathbf{2_32_22_1})T_1(4_32_1)$	$Fe_6Q_6(PR_3)_4L_2$, $[Fe_6Q_6(PEt_3)_6]^{1+}$	46
$M_6Q_9L_2$ (**12**)	$T_2(\mathbf{4_32_2})T_1(4_1)$	$[Fe_6Q_9(SR)_2]^{4-}$	47
$M_7Q_6L_7$ (**13**)	$T_2(\mathbf{4_33_2})T_1(4_33_2)$	$Fe_7S_6(PEt_3)_4Cl_3$	48
$M_8Q_6L_8$ (**14**)	$T_2(\mathbf{8_3})T_1(8_3)$	$[Fe_8S_6I_8]^{2-,3-,4-}$; $[Co_8S_6(SPh)_8]^{4-,5-}$	49; 50
$M_{18}Q_{30}$	$T_2(\mathbf{12_36_2})T_1(4_28_1)$	$[\alpha\text{-}Na_2Fe_{18}S_{30}]^{8-}$	27b
$M_{18}Q_{30}$	$T_2(\mathbf{8_310_2})T_1(4_32_24_1)$	$[\beta\text{-}Na_2Fe_{18}S_{30}]^{8-}$	27c
$M_{20}Q_{28}L_4$	$T_2(\mathbf{8_312_2})T_1(12_4)$	$[Mo_8Cu_{12}S_{32}]^{4-}$ (**18**)	51
$M_{20}Q_{38}$	$T_2(\mathbf{2_318_2})T_1(4_1)$	$[Na_9Fe_{20}Se_{38}]^{9-}$	27c, 52
$^1_\infty M_2Q_3$	$T_2(\mathbf{1_3})T_1(1_2)$	$^1_\infty[Fe_2Q_3]^{2-}$	36
$^2_\infty M_3Q_4$	$T_2(\mathbf{1_41_2})T_1(1_4)$	$^2_\infty WCu_2S_4$	53
$^2_\infty$MQ (**16**)	$T_2(\mathbf{1_4})T_1(1_4)$	$^2_\infty[CuQ]^{1-}$	54
$^3_\infty$MQ	$T_2(\mathbf{1_61_2})T_1(1_8)$	$^3_\infty MCu_3Q_4$[c,f]	55
$^3_\infty M_2Q$ (**17**)	$T_2(\mathbf{1_6})T_1(1_{20})$	$^3_\infty Cu_2Q$	56

[a] Polyhedra connectivity partitioning notation (see Appendix); reduced notation is shown in boldface. [b] Q = S, Se; L = $^-$SR, $^-$OAr, halide. [c] Q = S, Se, Te. [d] M = Mo, W. [e] M = V, Mo. [f] M = V, Nb, Ta.

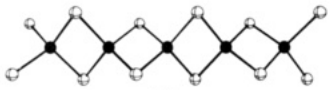

15

(1_2)-$^1_\infty MQ_2$

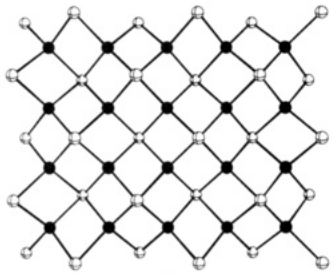

16

(1_4)-$^2_\infty$MQ

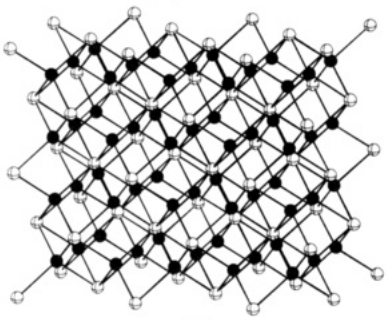

17

(1_6)-$^3_\infty M_2Q$

Figure 4. Structures and reduced PCP notation for extended solids consisting of infinite chains (**15**), sheets (**16**), and three-dimensional arrays (**17**) of edge-sharing MQ_4 tetrahedra. Specific examples are given in Table 2. Figure 5 shows a stereoview of **17** which is the antifluorite structure.

the former by extending the edge-sharing CdI_6 octahedra in a third dimension. An equally likely pitfall is in the overgeneralization of a structural theme. For example, while the subfamily of metal–copper–chalcogenides found in Table 2 can be adequately modeled with the antifluorite structure, a significantly more efficient candidate exists. All of these heterometallic structures may be simply described as tetrathiometalates which are sometimes bridged by tetrahedrally coordinating copper atoms. The degree of connectivity of the copper-centered tetrahedra is never greater than two. Extension of these more specific structural criteria leads to a three-dimensional parent solid with formula MCu_3Q_4 and a unit cell whose corners are defined by the Mo atoms in the cluster $[Mo_8Cu_{12}S_{32}]^{4-}$,[51] **18** (black and gray spheres represent Mo and Cu, respectively). These and other suggested parent solids are collected in Table 3.[4,9b,61] The method described here is just as readily applied to these systems as to the iron-chalcogenides.

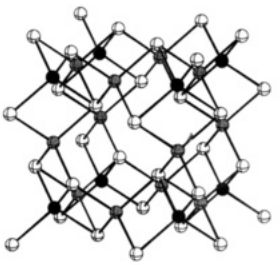

18

Generating Fragments

Having constructed a suitable parent solid, its potential as a cluster source may now be exploited by extricating the appropriate pieces, or *fragments*, of the structure. Upon translation into clusters, these fragments will, by design of the parent solid, fulfill the criteria for membership in the original cluster family. Here

(61) (a) Martinengo, S.; Ciani, G.; Sironi, A.; Chini, P. *J. Am. Chem. Soc.* **1978**, *100*, 7096. (b) Süss-Fink, G. *Angew. Chem., Int. Ed. Engl.* **1991**, *30*, 72 and references therein.

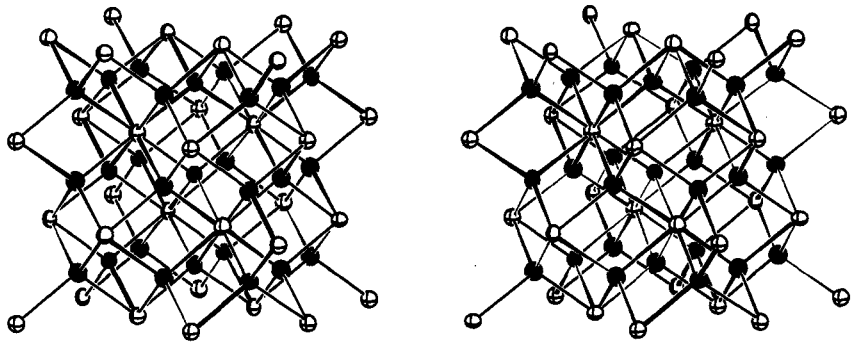

Figure 5. Stereoview of the antifluorite structure, M_2Q (**17**), consisting of an fcc lattice of Q atoms with M atoms occupying all of the tetrahedral holes. Each chalcogen is coordinated by eight metal atoms in a cubic arrangement.

Table 3. Suggested Parent Solids for Some of the More Extensive Cluster Families

	parent solid	
cluster family	PCP descriptor	structure
Δ_0-benzenoids	$\Delta_0(2_3)$–$^2_\infty$C	graphite
Δ_1-borazines	$\Delta_1(1_6)$–$^2_\infty$BN	BN
T_0-alkanes	$T_0(1_4)$–$^3_\infty$C	diamond
T_1-silicates	$T_1(1_{12})$–$^3_\infty$SiO	zinc blende
T_2-iron chalcogenides	$T_2(1_6)T_1(1_{16})$–$^3_\infty Fe_2Q$	antifluorite
T_2-metal–copper chalcogenides	$T_2(1_6)\|T_2(1_2)T_1(1_8)$–$^3_\infty MCu_3Q_4$	VCu_3S_4
$SPy_{2,1}$-polyoxovanadates	$SPy_2(1_2)SPy_1(1_3)$–$^2_\infty V_2O_5$	V_2O_5[9b]
$O_{2,1}$-polyoxometallates	$O_2(1_{12})O_1(1_6)$–$^3_\infty$MO	rock salt
O_2-iodoantimonates	$O_2(1_{12})O_1(1_6)$–$^3_\infty$SbI	rock salt
P_0-metal carbonyls	$P_0(1_{12})$–$^3_\infty M^a$	close packed[4,61]

[a] P = CO or ACO for a surrounding packing of order ABC or ABA, respectively.

we address the problem of accessing all such distinct fragments contained within a parent solid. A recursive procedure for the generation and subsequent enumeration of edge-sharing antifluorite fragments is described in detail.

Lattice Animals. Recognition of all possibilities for any sizable fragment of a three-dimensional solid presents a task of immense proportion—one that rapidly becomes immoderate for even the most advanced computers. It is therefore helpful (perhaps even unavoidable) to introduce the simplification of replacing structures with graphs. For polyhedra-based structures, it is generally most efficient to represent the metal-centered polyhedra with points and the essential vertex-sharing connections with lines.[62] Accordingly, in the antifluorite structure (**17**), each MQ_4 tetrahedron is replaced by a point and each edge shared between neighboring tetrahedra by a connecting line. The result is the simple cubic lattice of connected points shown at the top in Figure 6. Rather than generating fragments of the actual solid, the simpler exercise of deriving animals from the lattice may be undertaken. The animals derived correspond to the desired fragments. Thus, animals originating from our cubic lattice correspond to antifluorite fragments composed exclusively of edge-sharing tetrahedra. Nine (**2–4, 6, 8, 10, 11, 13,** and **14**) of the thirteen clusters displayed in Figure 3 are immediately recognizable as directly related to fragments of the antifluorite structure.[63] Figure 6 shows how their graphs may be extracted from the simple cubic lattice. The basis for our reduced PCP notation is now evident. By discarding all but the edge-sharing (T_2) connectivity partitions, the descriptive notation for a cluster (Figure 3) is reduced to precisely that of its corresponding graph (Figure 6). Similarly

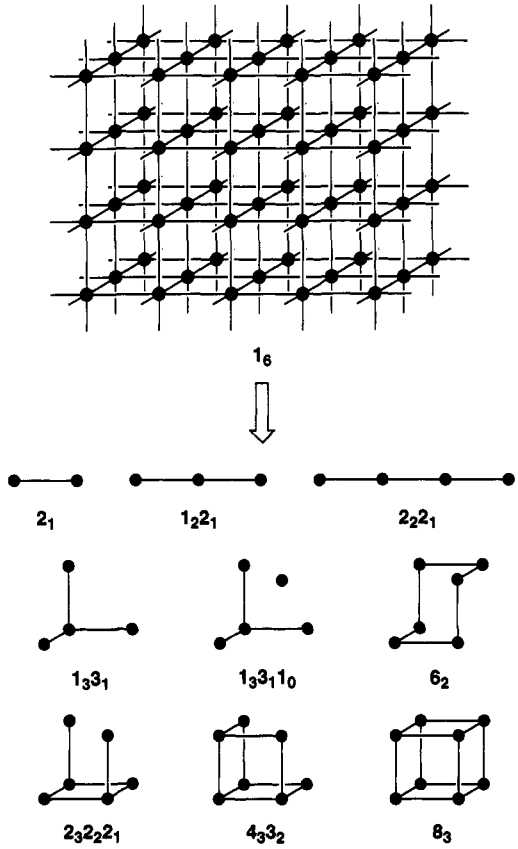

Figure 6. The antifluorite parent lattice **17** and animals[63] derived from it which are graphical representations of certain clusters depicted in Figure 3. Points represent MX_4 (X = Q or L) tetrahedra and lines represent their shared edges. Note the exact correspondence between the points in the graphs shown here and the metal sites in the related compounds shown in Figures 3 and 4.

for other systems, a reduced PCP notation should become apparent upon identification of the essential vertex-sharing situations and establishment of a graphical representation.

Formulae for counting lattice animals are, to the best of our knowledge, completely unknown, and their enumeration on even a square lattice remains an open problem.[64] We must therefore resort to a recursive procedure in which the animals of order m (i.e., containing m points) are generated by adding a point in all possible ways to each animal of order $m - 1$ and eliminating duplicates. Once a suitable coordinate system has been selected, an animal can be defined as a collection of lattice points $\{(x_1,y_1,z_1); (x_2,y_2,z_2); \ldots; (x_m,y_m,z_m)\}$ along with its adjacency matrix. For a simple cubic lattice, the Cartesian system may be employed

(62) In some cases it is possible to further simplify the situation by replacing a group of atoms with a single point. For example, a benzenoid graph might represent a C_6 ring by a point and an edge (C–C bond) shared between two neighboring rings by a line joining the points.

(63) The $1_33_11_0$ graph (corresponding to cluster **8**) contains an isolated point, and is therefore not an animal. This exception is discussed in more detail below.

(64) Soteros, C. E.; Whittington, S. G. *J. Math. Chem.* **1990**, *5*, 307.

Table 4. Number of Animals, Trees, Polycubes, and Fragments Generated from the Simple Cubic Lattice and the Antifluorite Structure

m	animals	trees	polycubes	fragments[a]
2	1	1	1	1
3	2	2	2	2
4	9	8	8	9
5	37	35	29	29
6	275	240	166	165
7			1023	962
8			6922	6423

[a] Chiral fragments counted only once.

such that coordinates (x_i,y_i,z_i) of the lattice points are restricted to integers, and the distance between any two *neighboring* points is then unity. Given the set $\mathbf{A}_{m-1}$ of all animals of order $m-1$, the set $\mathbf{A}_m$ of animals of order m is constructed as follows. From each distinct animal in $\mathbf{A}_{m-1}$, animals of order m are created by adding a new neighboring point,

$$(x_m,y_m,z_m) \in \{(x_i\pm1,y_i,z_i);\ (x_i,y_i\pm1,z_i);\ (x_i,y_i,z_i\pm1)|i = 1, ..., m-1\} \quad (3)$$

and modifying the adjacency matrix such that it is joined to point i. The new animal is then compared with the animals already in $\mathbf{A}_m$. All equivalent orientations (attained via rotations of 90° about the x, y, and z axes) are checked for every possible choice of origin (achieved by translating the entire graph by $(-x_i,-y_i,-z_i)$ for all points, i). If a perfect match is found, the animal is not new and is rejected. Otherwise, it is added to $\mathbf{A}_m$, along with any additional animals obtained by further connecting point m with neighboring points other than i (this final step is omitted when generating trees). All that remains is to declare a starting point, for which we may take the set $\mathbf{A}_1$ containing a solitary animal $\{(0,0,0)\}$ with no joining lines. Table 4 lists the number of distinct trees and animals of order 6 or less generated by implementing the described procedure on a computer.

Not all animals correspond to actual solid fragments. Some animals contain neighboring points that are not connected, whereas in the parent solid, all neighboring polyhedra are, by definition, connected. As an example, consider the two animals diagrammed in **19**. The points contained in both are representative of the four

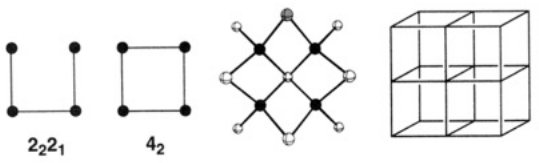

19

metal-centered tetrahedra in the antifluorite fragment displayed. However, the leftmost animal ($\mathbf{2_2 2_1}$) is missing a line between two neighboring points, implying that the tetrahedra corresponding to these points should not share a common edge. This entails replacing the shaded Q atom with two terminal ligands L, one bound to each metal. Although the resulting cluster has some leeway for distortion, its predicament is stereochemically unfavorable owing to steric interactions between the added ligands, which project from their M atoms in the same direction. We therefore discard any animals with this condition, keeping only those in which all neighboring points are joined (i.e., those corresponding to actual fragments of the parent solid). In so doing, our task of generating fragments is simplified enormously. Because it is assumed that all neighboring points in an animal are connected, adjacency matrices are unnecessary, and only the coordinates need be generated and compared. For a simple cubic lattice, this subset of "fragment" animals is isomorphic to the set of polycubes. The three-dimensional equivalent of a polyomino,[65] a *polycube* of order m, is a solid figure formed by fusing the faces of m unit cubes.[66] Since the cubes are space-filling, all nearest neighbors must be connected by a face, as demonstrated in **19** with the tetracube depicted on the right. Subsequently, an animal only corresponds to a polycube if all of its neighboring points are connected. Although the animal with four lines ($\mathbf{4_2}$) in **19** corresponds to the tetracube containing four face-sharing connections, the $\mathbf{2_2 2_1}$ animal has no polycube counterpart. Thus, the cubes and their shared faces are exactly equivalent to the points and lines used to represent tetrahedra and shared edges in our antifluorite fragments. The polycubes are also enumerated in Table 4. As expected, their numbers are significantly diminished from the total number of animals. While mirror-image animals are considered distinct (both images are counted in the enumerations of Table 4), enantiomeric clusters are not (at least for our purposes). Since chiral animals correspond to chiral fragments, one member of each pair of mirror-image animals is eliminated in order that both fragment enantiomers are not created. This is accomplished by introducing a mirror plane when checking different orientations in the comparison stage of animal generation.

Fragments. Once the relevant animals have been generated, they are then converted into fragments. Depending on the organization of the parent solid, an animal may have more than one fragment associated with it. Such is the case for some of our antifluorite fragment animals. Suppose we apply one iteration of the above animal-generating algorithm to the $\mathbf{4_2}$ animal in **19**. One of the two distinct animals that result is the $\mathbf{1_3 3_2 1_1}$ animal shown at the left in **20**. To convert this animal into a fragment, simply choose a spot in the antifluorite structure, overlay the animal so that points coincide with metal centers, and cut out these metals along with any attached chalcogenide atoms. If we overlay it in the lower front left corner of one of the antifluorite representations (either Figure 4 or 5) the result is the M_5Q_{11} fragment depicted in the middle of **20**. However, if we translate

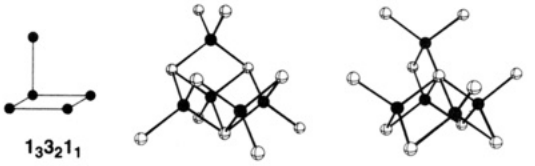

20

the animal an odd number of metal centers in any direction and then overlay it (say in the lower front *right* corner), a different M_5Q_{11} fragment is obtained, namely that shown at the right in **20**. At most, two distinct fragments may be obtained by overlaying any given animal at all possible sites in the antifluorite structure. This phenomenon arises from a lack of inversion symmetry at the tetrahedral metal centers. When the entire structure **17** is inverted around a single metal center, the "new" structure is, of course, exactly equivalent to the original. However, now the local environment around that center and around an animal overlayed on that center is different. The effect is the same as translating the structure (or the animal) an odd number of metal centers in any direction. For some animals (particularly three-dimensional animals) the inversion of the MQ_4 tetrahedra centered at each point leads to a new fragment, as is the case in **20**, while for others it does not, as in **19**. Two fragments or clusters so related are called *invertomers*.

In practice, antifluorite fragments may be generated from the animals by a more direct method than that just described. The integral coordinates of the points in an animal can be taken as the unscaled coordinates for metal atoms. Coordinates for all

(65) A *polyomino* of order m is a two-dimensional entity formed by fusing the edges of m coplanar unit squares: Martin, G. E. *Polyominoes*; The Mathematical Association of America: USA, 1991.

(66) Gardner, M. *Sci. Am.* **1972**, *227*, 176.

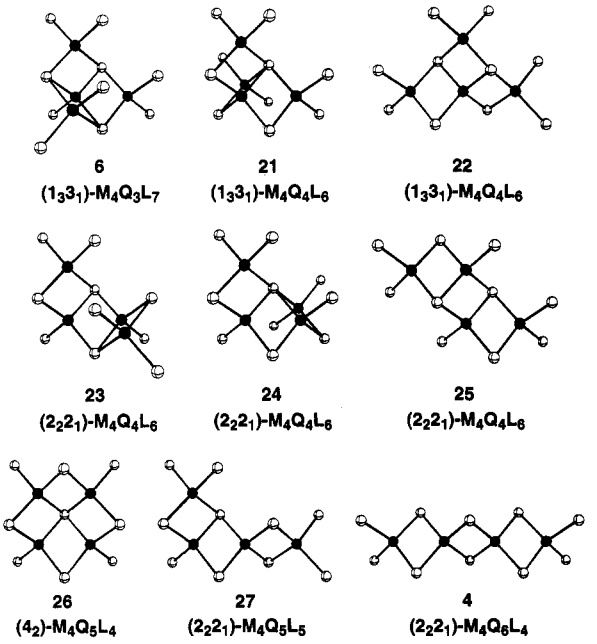

Figure 7. Clusters corresponding to the nine distinct antifluorite fragments based on four edge-sharing MQ_4 tetrahedra.

attached Q sites may then be generated locally from each metal position (x_i,y_i,z_i) in turn. This yields two sets of coordinates, Q_+ and its "inverse" Q_-, corresponding to two possibly different fragments, which may be expressed as

$$Q_\pm = \{(x_i,y_i,z_i) \pm (^1/_2)(\sigma_x,\sigma_y,\sigma_z) | i = 1, ..., m\} \quad (4)$$

where

$$(\sigma_x,\sigma_y,\sigma_z) \in \{(\sigma,\sigma,\sigma); (\sigma,-\sigma,-\sigma); (-\sigma,\sigma,-\sigma); (-\sigma,-\sigma,\sigma) | \sigma = (-1)^{(x_i+y_i+z_i)}\} \quad (5)$$

The combined set $Q_\pm$ actually generates a cube of eight coordinating atoms around each metal center.[67] The vectors $+(^1/_2)(\sigma_x,\sigma_y,\sigma_z)$ allocate four atoms from each cube into a tetrahedron (the union of which comprise Q_+), leaving an inverted tetrahedron of remaining atoms allocated by the vectors $-(^1/_2)(\sigma_x,\sigma_y,\sigma_z)$ (their union comprising Q_-). Q_+ and Q_- are compared using the same procedure employed on animals above, and any duplicates are discarded. Finally, all coordinates (M and Q) are multiplied by an appropriate scaling factor (ca. 2.6 Å for M = Fe and Q = S) resulting in a complete set of atomic positions for each fragment. These fragments are enumerated in Table 4. Note that the additional "inverse" fragments are roughly counterbalanced by the exclusion of one enantiomer from each pair, leading to comparable numbers for polycubes and fragments.

Clusters. Translating fragments into clusters is a simple matter of changing the Q atoms that are bonded to only one metal center into L atoms and adjusting the stoichiometries accordingly.[68] For example, the two M_5Q_{11} fragments in **20** would translate into $M_5Q_5L_6$ and $M_5Q_6L_5$ clusters (from left to right, respectively). The mapping from fragments to clusters is, of course, one-to-one, and consequently the fragment enumeration in Table 4 also holds for the corresponding clusters. Thus, the nine distinct fragments containing four metals translate into nine distinct clusters (Figure 7). Clusters **4** and **6** are members of our original family. The

(67) Applying $Q_\pm$ engenders a set of structures built up from face-sharing MQ_8 cubes, corresponding to fragments of a parent solid (MQ) with the cesium chloride structure. If chiral animals are not excluded, this set is isomorphic to the set of polycubes.

(68) If a particular terminal ligand has been decided upon, the appropriate modifications should also be made to the L atom coordinates.

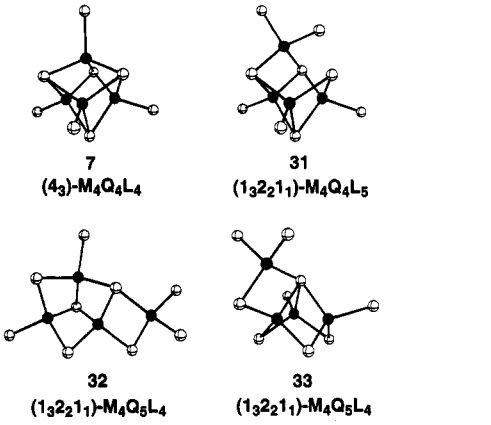

Figure 8. All of the distinct four-metal clusters derived by applying the folding process to the nine clusters in Figure 7.

structure of **22** is that adopted by the tetrathiomolybdate- and tetrathiotungstate-based clusters $[MCu_3S_4(S_2CNEt_2)_3]^{2-}$, where M = Mo, W is the central 1_3 metal.[41] Cluster **26** corresponds to the M_4Q_9 fragment in **19** and consists of a square metallic arrangement, already established structurally as the core in the cluster $[Cu_4(ettu)_9]^{4+}$ (ettu = ethylenethiourea).[69] (Note the absence of the cubane structure **7**, which does not directly correspond to a fragment of the antifluorite structure.) The resulting clusters are compiled to form the initial structural database, which has been generated by execution of steps 1–5 in Figure 2.

Cluster Rearrangements

Members of the initial database may be subjected to a variety of structural rearrangements, generating still further eligible clusters. The different rearrangement processes have been classified as folding, closure, fusion, and condensation. These rearrangements are not necessarily intended to suggest possible reaction or formation pathways, but rather to produce new cluster structures from those afforded by the above protocol. Each is described in general terms and then applied to the iron–chalcogenide cluster family. When practicable, computer-based algorithms are employed to facilitate the process. All of the new clusters which result are entered in the database, producing a much more comprehensive collection of structures. These procedures constitute step 6 in the flow chart of Figure 2.

Folding. Cutting a fragment out of the parent solid creates potential vertex-sharing situations on at least the peripheral metal centers. Depending on the specifics of its geometry, it may be possible for the corresponding cluster to collapse in such a manner as to join some of these centers without distorting their polyhedral environment. This intracluster process is called *folding*. The various modes of flexing must be rigorously tested with rigid polyhedra, until all of the structural motifs giving rise to a successful fold have been recognized. Not every cluster can be folded, and in extreme cases, an entire family of clusters may prove nonpliant. In general, systems with face-sharing polyhedra are not amenable to folding.

Only one folding motion is compatible with the structural features exhibited by the clusters derived from antifluorite fragments. The process involves the formation of three-metal rings by merging two proximal edges which already have one Q atom in common. The motif required has the structure shown at the left in **28**, which depicts the simplest possible fold. Here, an $M_3Q_3L_5$ cluster is folded over so that the two shaded L atoms coalesce into a single Q atom, thereby generating a new cluster which is not directly related to a piece of the antifluorite structure. The new cluster is actually **5**, and it contains one of the anomalous

(69) Crumbliss, A. L.; Gestaut, L. J.; Rickard, R. C.; McPhail, A. T. *J. Chem. Soc., Chem. Commun.* **1974**, 545.

μ_3-Q atoms mentioned above. These symmetrical μ_3 bridges are a direct result of folding. Each fold is also accompanied by a change in stoichiometry, of which there are three possibilities, depending on whether the atoms coalescing are Q or L or both:

$$M_mQ_qL_l \rightarrow \begin{cases} M_mQ_{q-1}L_l \\ M_mQ_qL_{l-1} \\ M_mQ_{q+1}L_{l-2} \end{cases} \quad (6)$$

In all cases, cluster nuclearity (m) is unaffected and the total number of nonmetals ($q + 1$) is reduced by one. As we shall see, this folding process is by far the most important type of rearrangement for Fe–Q clusters.

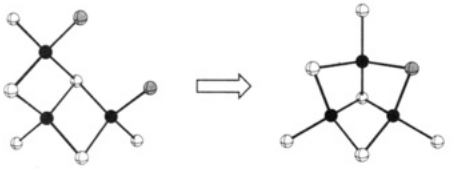

28

Computationally, it is more convenient to fold animals than their corresponding clusters. The features required for a graph to be capable of folding are those exemplified by the freshly cut $\mathbf{1_22_1}$ animal at the left in **29**. Here, dangling connections

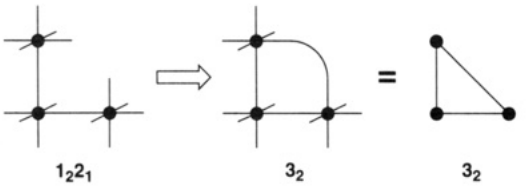

29

(tetrahedral edges) are represented by the additional lines. Two of these lines are in much closer proximity than is typically observed, and connecting them produces a new animal, $\mathbf{3_2}$. The presence of a similar situation in any animal gives rise to a potential fold, which may then be indicated by a diagonal line joining the points involved (as illustrated on the right in **29**). The operation in **29** is, of course, exactly analogous to that performed on clusters in **28**. Some animals can be folded more than once, and multiple folds are in fact necessary to derive the remaining three members of our original cluster family. The folded animals in **30** correspond to clusters **7**, **9**, and **12**, from left to right, respectively.

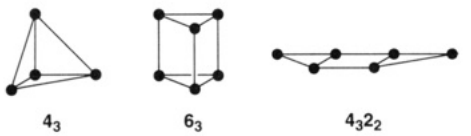

30

In generating folded clusters, the computer merely searches for animals containing the open triangular motif (**29**) and makes the additional connection. Subsequent translation of the graphs into clusters again yields two different structures for some animals. The folded clusters are then compared with those previously obtained, and duplicates are discarded. Typically, each folded cluster may be obtained by folding more than one structure, and therefore duplicates are frequent. For example, suppose we apply our folding process to the M_4 clusters in Figure 7. Only four distinct new clusters (Figure 8) arise. Both **6** and **23** fold once to produce the same cluster, **31**. Similarly, **21** and **24** both fold up into **33**, and three different clusters (**22**, **25**, and **27**) all yield **32** upon folding. Folding **31** again (i.e., folding **6** and **23** twice) results in the cubane structure, **7**. Clusters **4** and **26** do not contain any proximal unshared edges, and consequently cannot be folded. All of the new folded clusters are added to the database. In some instances, folding an animal locks the structure of the corresponding cluster in a conformation that prohibits implementation of certain subsequent folds. For a precise enumeration, all such situations must be recognized and the appropriate animals discarded. Unfortunately, the structural complexity at higher nuclearities precludes any straightforward solution to the problem, and for $m > 6$, a *small* percentage of the folded animals generated do not correspond to actual clusters. The fictitious structures which result have formulae with $(q + l) < 2m$ (i.e., they derive from animals containing a large number of cycles), and are only identified upon individual examination. Consequently, "enumeration" for these stoichiometries merely provides an upper bound until a more focused inspection is warrented, lending an evolutionary aspect to this portion of the database.

Table 5. Some Hypothetical One-Dimensional Chains and Examples of Their Cyclic Cluster Derivatives

chain	cyclic clusters	ref
$L_1(1_2)$–$^1_\infty Ag(SR)$[a]	$L_1(12_2)$–$Ag_{12}(SCy)_{12}$[b]	70
$\Delta_0(1_2)$–$^1_\infty CL$[a]	$\Delta_0(m_2)$–C_mH_m; m = 4, 6, 8, 10, 12, 16, 18	71
$\Delta_1(1_2)$–$^1_\infty[BO_2]^{1-}$[a]	$\Delta_1(3_2)$–$[B_3O_6]^{3-}$	72
$S_1(1_2)$–$^1_\infty Cu(OH)L_2$	$S_1(8_2)$–$Cu_8(OH)_8(dmpz)_8$[c]	73
$S_2(1_2)$–$^1_\infty Ni(SR)_2$	$S_2(m_2)$–$Ni_m(SR)_{2m}$; m = 4, 5, 6, 8	74
$T_0(1_2)$–$^1_\infty CL_2$[a]	$T_0(m_2)$–C_mH_{2m}; m = 3–16, ...	71
$T_1(1_2)$–$^1_\infty[PO_3]^{1-}$[a]	$T_1(m_2)$–$[P_mO_{3m}]^{m-}$; m = 3–8	75
$T_1(1_2)$–$^1_\infty[SiO_3]^{2-}$[a]	$T_1(m_2)$–$[Si_mO_{3m}]^{(2m)-}$; m = 3, 4, 6, 8, 9, 12	76
$T_1(1_3)$–$^1_\infty[Si_2O_5]^{2-}$	$T_1((2n)_3)$–$[Si_{2n}O_{5n}]^{(2n)-}$; n = 3–6	76
$T_2(1_2)T_1(1_2)$–$^1_\infty[Fe_2S_2L_2]^{1-}$ (**34**)	$T_2(6_2)T_1(6_2)$–$[Fe_6S_6Cl_6]^{3-}$ (**10**)	45
$T_2(1_2)T_1(1_2)$–$^1_\infty$GaSL (**34**)	$T_2(m_2)T_1(m_2)$–$Ga_mS_m(^tBu)_m$; m = 6 (**10**), 8 (**35**)	77
$SPy_1(1_2)$–$^1_\infty[ReCl_4]^{1-}$	$SPy_1(3_2)$–$[Re_3Cl_{12}]^{3-}$	78
$O_1(1_2)$–$^1_\infty[TiOL_4]^{1-}$	$O_1(4_2)$–$[Ti_4O_4(NTA)_4]^{4-}$[d]	79
$O_2(1_2)$–$^1_\infty Fe(OR)_2L_2$	$O_2(10_2)$–$Fe_{10}(OMe)_{20}$-$(O_2CCH_2Cl)_{10}$	80

[a] Structural evidence indicates the existence of related chains in the solid state. [b] Several Ag atoms display a coordination geometry intermediate to linear and trigonal planar. [c] Hdmpz = 3,5-dimethylpyrazole. [d] NTA = nitrilotriacetate.

Closure. Imposing appropriate boundary conditions on an infinitely extended structure can lead to a finite, yet topologically equivalent structure. This operation is called *closure*, and for the purpose of cluster generation, it may be usefully applied to structures extending in either one or two dimensions. These two distinct processes are termed *chain cyclization* and *sheet wrapping*, respectively.

The chain cyclization process involves isolating a suitable repeat unit from within a periodically extended chain structure, looping its two ends around and joining them in a fashion concordant with their original connectivity. Thus, a chain may yield cyclic clusters of varying size, depending upon the length of the repeat unit. Table 5 lists some known clusters with structures that may be derived by cyclizing a one-dimensional chain (real or hypothetical).[70–80] The broad range of chemical systems and

(70) Dance, I. G. *Inorg. Chim. Acta* **1977**, *25*, L17.
(71) Streitweiser, A.; Heathcock, C. H. *Introduction to Organic Chemistry*; Macmillan: New York, 1985; pp 77–87.
(72) Schneider, W.; Carpenter, G. B. *Acta Crystallogr.* **1970**, *B26*, 1189.
(73) Ardizzoia, G. A.; Angaroni, M. A.; La Monica, G.; Cariati, F.; Moret, M.; Masciocchi, N. *J. Chem. Soc., Chem. Commun.* **1990**, 1021.
(74) (a) Gaete, W.; Ros, J.; Solans, X.; Font-Altaba, M.; Briansió, J. L. *Inorg. Chem.* **1984**, *23*, 39. (b) Woodward, P.; Dahl, L. F.; Abel, E. W.; Crosse, B. C. *J. Am. Chem. Soc.* **1965**, *87*, 5251. (c) Gould, R. O.; Harding, M. M. *J. Chem. Soc. A* **1970**, 875. (d) Dance, I. G.; Scudder, M. L.; Secomb, R. *Inorg. Chem.* **1985**, *24*, 1201.

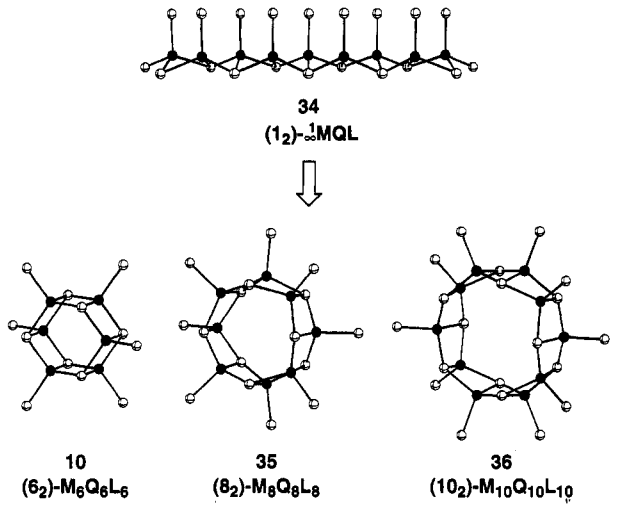

Figure 9. Cyclization of a one-dimensional chain of edge-sharing tetrahedra (**34**) to form the series (m_2)-$M_mQ_mL_m$ where m = 6 (**10**), 8 (**35**), 10 (**36**), etc. The core structure of each cyclic cluster consists of interlocking regular $(m/2)$-gon antiprisms of M and Q atoms.

polyhedra represented in these examples underscores the utility of chain cyclization as a tool in both the description and generation of cluster structures. Typically, chains befitting cyclization are readily derived from the parent solid. The simplest such chain fragment of the antifluorite structure is **15**, which upon cyclization affords a series of clusters with formulae (m_2)-M_mQ_{2m} where m is even (all possible repeat units in **15** contain an even number of metals). The $M_{14}Q_{28}$ member in this series forms the peripheral basis for the clusters $[\alpha,\beta\text{-}Na_2Fe_{18}S_{30}]^{8-}$,[27b,c] and recently a similar cluster, $[Fe_{14}Te_{22}]^{6-}$,[81] based on the smaller $M_{10}Q_{20}$ member has been described. Given the rather poor flexibility of the parent chain, the formation of structures containing members with fewer than ten metals seems unlikely.

For a thorough compilation of structures, it is necessary to transcend the constraints implicit in the parent solid and consider possible alternative structural sources. Flexible chains that do not derive from the parent solid but are capable of cyclizing into low nuclearity clusters can often be constructed. An example is illustrated in Figure 9. Stringing tetrahedra together by edges in one direction on a flat surface results in a chain (**34**), which is not a fragment of the antifluorite structure. Due to the extremely close interactions it imposes between metal centers, the chemical stability of such a chain structure is problematic. However, the strain is alleviated with cyclization, wherein a series of clusters with formulae (m_2)-$M_mQ_mL_m$ (m even) is formed. Of this series, the smallest member (m = 6) corresponds to the prismane cluster (**10**) already generated directly from an antifluorite fragment, while the remainder consist of new structures that are added to the database. The structure of **35** (m = 8) has been proposed for $Ga_8S_8(^tBu)_8$ based on ^1H NMR and mass spectral data.[77] The formation of higher nuclearity members in this series should be less favorable, because with increasing m, the metal centers are forced closer and closer together as the structures approach that of **34** (m = ∞).

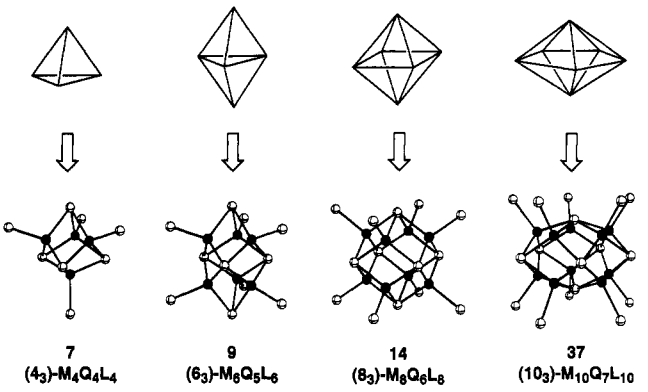

Figure 10. Sheet $((1_3)$-$^2_\infty M_2QL_2)$ wrapping of regular deltahedra (tetrahedron, trigonal bipyramid, octahedron, and pentagonal bipyramid) to form closed clusters.

Sheet wrapping, the two-dimensional analogue of chain cyclization, involves extracting pieces from a two-dimensional sheet and wrapping them around to form closed structures with no exposed edges. Sheets are much less pliant than chains, and consequently sheet wrapping is usefully applied to far fewer cluster systems than chain cyclization. One unusually extensive example, however, is embodied in the fullerenes, all of whch can be formed by closing up pieces cut from a single layer of graphite. None of the edge-sharing sheets inherent in the antifluorite structure (e.g. **16**) have the degree of flexibility required for wrapping. As with chains, it is possible to construct sheet structures amenable to wrapping, but unrelated to the parent solid. For example, a sheet, (1_3)-$^2_\infty M_2QL_2$, may be assembled by a close packing of tetrahedra on a flat surface (i.e., by extending **34** in a second dimension), such that the Q atoms at the tetrahedral bases form a regular triangular lattice. Pieces of this sheet may be wrapped to enclose any regular deltahedron, producing clusters in which each vertex is a Q atom and each face is capped by a normal ML moiety. Figure 10 displays the results of wrapping the smallest four deltahedra. Clusters **7**, **9**, and **14** (corresponding to a wrapped tetrahedron, trigonal bipyramid, and octahedron, respectively) are all original members of the Fe–Q cluster family that have been derived by previously described methods. Wrapping larger deltahedra yields new clusters, such as **37**, which are added to the database, along with derivatives obtained by extracting tetrahedra. Once again, the larger clusters should be less stable due to crowding of their metal centers.

Fusion. It is sometimes possible to form relevant new structures by merging two database clusters with complementary features. When two such clusters are merged by superposing one or more of their atoms, the process is called *fusion*. In general, the most appropriate way of performing this coupling employs the prevalent type of vertex-sharing interaction. For Fe–Q clusters, the operation would involve fusing tetrahedral edges. Since any reasonable structures so generated are, at least for small m, already members of our database, this avenue is not pursued here.

Occasionally, two or more clusters will have matching structural motifs that enable them to be rigidly fused by some means other than the principal vertex-sharing interaction. An example is provided in Figure 11. Here, the three L atoms at the top of **6** form an open triangular face that meshes perfectly with similar triangular faces found in other clusters. Fusion of **6** at this interface with an ML_4 tetrahedron, **5**, and another **6** generates clusters **8**, **38**, and **39**, respectively. In all three of these structures, the two halves are linked by corner-sharing (T_1) interactions. A member of our original family, cluster **8** is directly related to a fragment of the antifluorite structure. As this fragment is only partially based on edge-sharing tetrahedra, **8** was not derived in the above treatment. The structure of **38** is exactly that adopted by $Ga_7S_7(^tBu)_7$.[77] Cluster **39** is a tetrahedral, all-iron version of the FeMo–cofactor cluster of nitrogenase, as recently resolved

(75) (a) Kalliney, S. Y. *Top. Phosphorus Chem.* **1972**, *7*, 255. (b) Schülke, U.; Averbuch-Pouchot, M. T.; Durif, A. *Z. Anorg. Allg. Chem.* **1993**, *619*, 374.

(76) Liebau, F. *Structural Chemistry of Silicates*; Springer-Verlag: Berlin, 1985.

(77) (a) Power, M. B.; Ziller, J. W.; Tyler, A. N.; Barron, A. R. *Organometallics* **1992**, *11*, 1055. (b) Power, M. B.; Ziller, J. W.; Barron, A. R. *Organometallics* **1992**, *11*, 2783.

(78) Bertrand, J. A.; Cotton, F. A.; Dollase, W. A. *Inorg. Chem.* **1963**, *2*, 1166.

(79) Wieghardt, K.; Quilitzsch, U.; Weiss, J.; Nuber, B. *Inorg. Chem.* **1980**, *19*, 2514.

(80) Taft, K. L.; Delfs, C. D.; Papaefthymiou, G. C.; Foner, S.; Gatteschi, D.; Lippard, S. J. *J. Am. Chem. Soc.* **1994**, *116*, 823.

(81) Roof, L. C.; Kolis, J. W. *Chem. Rev.* **1993**, *93*, 1037.

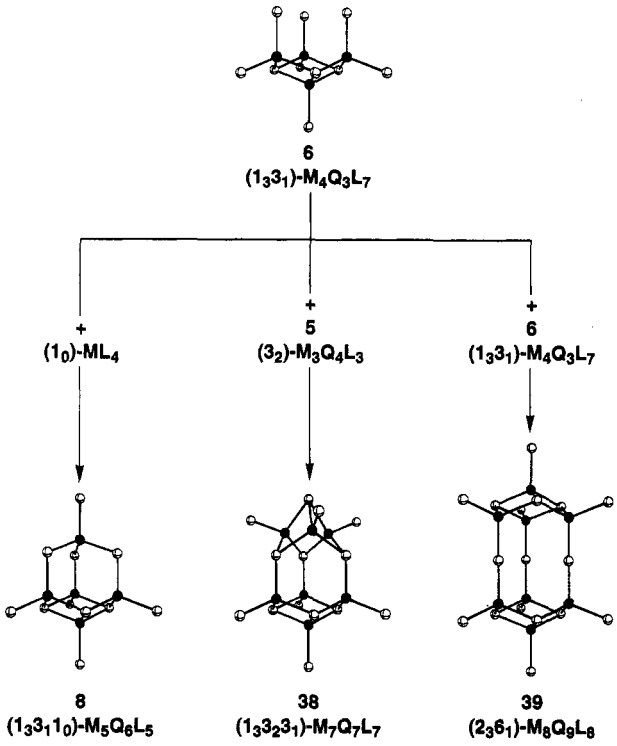

Figure 11. Fusion of **6** with an ML_4 tetrahedron, **5**, and **6** to form compact new clusters based on two edge-sharing halves linked by three common corners.

crystallographically.[82] This cluster has considerable flexibility about its waist, allowing the three strictly corner-shared Q atoms to splay outward, while simultaneously drawing their attendant metal centers closer together. The distribution of Fe–Fe contacts in the cofactor[82,83] cannot, however, be attained in this fashion, and it is only achievable by enforcing the observed trigonal planar environment about the six symmetry-related iron atoms.

Once a particular motif has been identified as well-suited for fusion, it is a trivial matter for the computer to search the database for clusters containing that motif and carry out all of their possible couplings. Implementing such a procedure with the triangular motif in **6** would give rise to a large number of new structures in which two halves are held together exclusively by corner-sharing. Given the lack of evidence for strict corner-sharing in Fe–Q clusters (even in the known examples of **8**, the corner-sharing metals are vanadium or molybdenum and not iron[42]), these structures are deemed *nonessential*, and the *fusion-generated clusters entered* in the database are limited to those displayed in Figure 11.

Condensation. When two clusters are merged by forging new bonds, the process is called *condensation*. An example is shown in Figure 12, in which two cuboidal $M_3Q_4L_3$ clusters (**5**) are condensed into a single $M_6Q_8L_6$ cluster (**40**). The two clusters mesh perfectly, facilitating the formation of six new M–Q bonds and an accompanying transition of the metal coordination from tetrahedral to square pyramidal. Although structure **40** is found in Fe–Q chemistry ($[Fe_6S_8(PEt_3)_6]^{2+,1+}$),[57] its metal centers do not conform to the tetrahedral condition imposed in defining our cluster family, and therefore, it is excluded from the database. Likewise, any structure produced by the condensation of two database clusters may be excluded on the grounds of containing either non-tetrahedral metals or X–X (X = Q, L) bonds. In general, depending on the rigidity of the cluster family constraints,

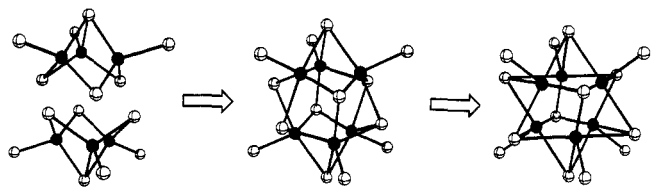

Figure 12. Condensation of two $M_3Q_4L_3$ clusters (left) to form a single $M_6Q_8L_6$ cluster (right). The middle structure is intermediate to the other two and shows the transition from tetrahedral to square pyramidal coordination of the metal centers.

it may be possible to generate suitable new structures via condensation.

The Cluster Database

When all of the possible cluster rearrangements have been exhausted, the new structures are compiled along with those derived directly from the parent solid, to form a comprehensive database of clusters. The database is then sorted (step 8 in Figure 2) by stoichiometry and whatever structural features are deemed appropriate for pinpointing clusters of particular interest.

Edge-Sharing Tetrahedral Clusters. As described in the preceding sections, we have employed a basis set of antifluorite fragments in extending the iron–chalcogenide cluster family. While the database developed was intended for use as a complete source of iron–chalcogenide cluster structures, in practice it serves equally well for *any* system based on edge-sharing tetrahedra, and hence the generalization to M, Q, and L. The clusters comprising this database are enumerated and, for $m \leq 6$, broken down by chemical formulae in Table 6. A surprisingly limited range of stoichiometries arise, with only 1, 3, 7, 11, and 21 different possibilities for m = 2–6, respectively. Consequently, at higher nuclearities ($m > 4$), more than one structural isomer exists for most stoichiometries, a general exception being the linear oligomers $M_mQ_{2m-2}L_4$ (see **2–4**). Table 6 also subdivides the total number of clusters into their methods of generation, sorting them as deriving from fragments or folding, with the remainder being attributable to other rearrangement processes. A "fragment" cluster with formula $M_mQ_qL_l$ corresponds to an actual antifluorite fragment with formula M_mQ_{q+1}. Note the large number of appropriate structures generated by folding as compared with the other rearrangement processes.

Sorting Clusters. The total number of database clusters increases sharply with the number of metal centers, m. For larger nuclearity clusters, this leads to an inordinate number of structures to sort through visually. It is, therefore, appropriate to impose certain restrictions that sort clusters of interest from the database. Two such restrictive criteria have already been recognized for the Fe–Q cluster family in the forms of uniterminal ligation and Q bridging modalities.[2] A cluster is *uniterminally ligated* if each metal center is coordinated by one or fewer terminal ligands (L). The simple empirical observation that all members of the original family with more than four metal centers are uniterminally ligated (in Figure 3, only **2**, **3**, **4**, and **6** are not) provides us with a rapid means for sorting through our database. Only a small fraction of the total number of clusters are uniterminally ligated. These are readily identified by the computer and separated from the other structures. The *bridging modality* (μ_n) of an atom Q is simply the number (n) of metals it shares bonds with, and it is generally limited to μ_2, μ_3, and μ_4 for lower nuclearity M–Q clusters. Notable exceptions include μ_5-S in $Ru_4WS_2(CO)_{13}(PMePh_2)$ and $Os_5WS(CO)_{19}(PPh_3)$, μ_6-S in $[Ni_8S(S^tBu)_9]^-$, and μ_8-S in $Cu_8S(S_2P(OC_2H_5)_2)_6$ and $[Rh_{10}S(CO)_{22}]^{2-}$.[13,58,84] At

(82) (a) Kim, J.; Rees, D. C. *Science* **1992**, *257*, 1677. (b) Chan, M. K.; Kim, J.; Rees, D. C. *Science* **1993**, *260*, 792. (c) Kim, J.; Woo, D.; Rees, D. C. *Biochemistry* **1993**, *32*, 7104.

(83) (a) Chen, J.; Christiansen, J.; Campobasso, N.; Bolin, J. T.; Tittsworth, R. C.; Hales, B. J.; Rehr, J. J.; Cramer, S. P. *Angew. Chem., Int. Ed. Engl.* **1993**, *32*, 1592. (b) Liu, H. I.; Filipponi, A.; Gavini, N.; Burgess, B. K.; Hedman, B.; Di Cicco, A.; Natoli, C. R.; Hodgson, K. O. *J. Am. Chem. Soc.* **1994**, *116*, 2418.

(84) (a) Adams, R. D.; Babin, J. E.; Natarajan, K.; Tasi, M.; Wang, J.-G. *Inorg. Chem.* **1987**, *26*, 3708. (b) Ciani, G.; Garlaschelli, L.; Sironi, A. *J. Chem. Soc., Chem. Commun.* **1981**, 563.

Table 6. Enumeration[a] of $M_mQ_qL_l$ Clusters Composed of Edge-Sharing Tetrahedra

formula	total	"fragments"[b]	folded	u. l. + μ_{2-4}[c]	examples
$M_2Q_2L_4$	1	1			**2**
$m = 2$	1	1			
$M_3Q_3L_5$	1	1			see **28**
$M_3Q_4L_3$	1		1	1	**5**
$M_3Q_4L_4$	1	1			**3**
$m = 3$	3	2	1	1	
$M_4Q_3L_7$	1	1			**6**
$M_4Q_4L_4$	1		1	1	**7**
$M_4Q_4L_5$	1		1		**31**
$M_4Q_4L_6$	5	5			**21–25**
$M_4Q_5L_4$	3	1	2	1	**26, 32, 33**
$M_4Q_5L_5$	1	1			**27**
$M_4Q_6L_4$	1	1			**4**
$m = 4$	13	9	4	2	
$M_5Q_4L_8$	3	3			
$M_5Q_5L_5$	2		2	1	**41**
$M_5Q_5L_6$	7	1	6		
$M_5Q_5L_7$	11	11			
$M_5Q_6L_4$	2		2	2	**42, 43**
$M_5Q_6L_5$	16	2	12	2	**8, 44, 58**
$M_5Q_6L_6$	9	9			
$M_5Q_7L_3$	2		2	1	**45**
$M_5Q_7L_4$	2		2		
$M_5Q_7L_5$	2	2			
$M_5Q_8L_4$	1	1			
$m = 5$	57	29	26	6	
$M_6Q_4L_{10}$	2	2			
$M_6Q_5L_6$	2		2	1	**9**
$M_6Q_5L_7$	1		1		
$M_6Q_5L_8$	5		5		
$M_6Q_5L_9$	11	11			
$M_6Q_6L_5$	1		1	1	**46**
$M_6Q_6L_6$	19	3	16	3	**10, 11, 47**
$M_6Q_6L_7$	51	10	41		
$M_6Q_6L_8$	51	51			
$M_6Q_7L_4$	3		3	1	**48**
$M_6Q_7L_5$	27		27	4	**49–52**
$M_6Q_7L_6$	68	22	46		**59**
$M_6Q_7L_7$	41	41			
$M_6Q_8L_3$	1		1		
$M_6Q_8L_4$	17	2	15	5	**53–57, 60**
$M_6Q_8L_5$	15	2	13		
$M_6Q_8L_6$	18	18			
$M_6Q_9L_2$	4		4	1	**12, 61**
$M_6Q_9L_4$	2		2		
$M_6Q_9L_5$	2	2			
$M_6Q_{10}L_4$	1	1			
$m = 6$	342	165	177	16	
$m = 7$[d]	2122	962	1151	69	
$m = 8$[d]	13185	6423	6755	257	

[a] For chiral clusters, only one enantiomer is counted. [b] Clusters directly derived from edge-sharing antifluorite fragments. [c] Uniterminally ligated with Q bridging modalities restricted to μ_{2-4}. [d] These numbers represent upper bounds; enumeration by formula available in Supplementary Material.

higher nuclearities, this tenet frequently breaks down,[85] although it remains as yet uncontested for M = Fe.[27b,c] Since the antifluorite structure contains exclusively μ_8-Q atoms, its sizable ($m \geq 5$) cluster progeny sometimes exhibit Q bridging modalities of μ_{5-8}. Given the preceding considerations, it is reasonable to disregard the majority of such structures, at least for $m \leq 10$.

Clusters that meet both the uniterminal ligation and Q bridging modality criteria are enumerated in Table 6. For $m = 2$, 3, and 4, there are zero, one (**5**), and two (**7**, **26**) such clusters, respectively. For $m = 5$ there are six: one (**8**) has been observed with iron, and the other five (**41–45**) are shown in Figure 13. Of these, only **44** was directly derived from an edge-sharing antifluorite fragment. Cluster **8** was generated by fusion (Figure 11), while the remainder resulted from single (**41**, **45**) and double (**42**, **43**) folds. The larger number of folded clusters fulfilling our conditions for selection is to be generally expected, since, as indicated above in eq 6, each fold has the potential to eradicate one or two terminal ligands (and therefore leads to more uniterminally ligated clusters). Precedent for structure **41** is found in the core geometry of $Zn_5(S^tBu)_5Me_5$.[86] The unsupported T_1 interaction in **44** is identical to that found in the handle of the basket cluster **11**. Such *basket-handle* bridges form the only means by which clusters with a reduced PCP descriptor $(...n_1)$ where $n > 0$ may achieve uniterminal ligation.[87] The database contains sixteen M_6 clusters that satisfy our restrictive criteria, including **9–12**. Those that are not members of the original Fe–Q cluster family (**46–57**) are depicted in Figure 14. Of these, two (**47**, **53**) were derived from fragments, and the rest resulted from one (**49**, **50**), two (**48**, **51**, **52**, **54–57**), or three (**46**) successive folds. Cluster **53** is a member (as is **26**) in a series of double chain clusters $((2n-4)_34_2)$-$M_{2n}Q_{3n-1}L_4$ with $n \geq 2$, all of which meet our criteria.[88] To date, no evidence has been reported suggesting the existence of any of the structures in Figure 14.

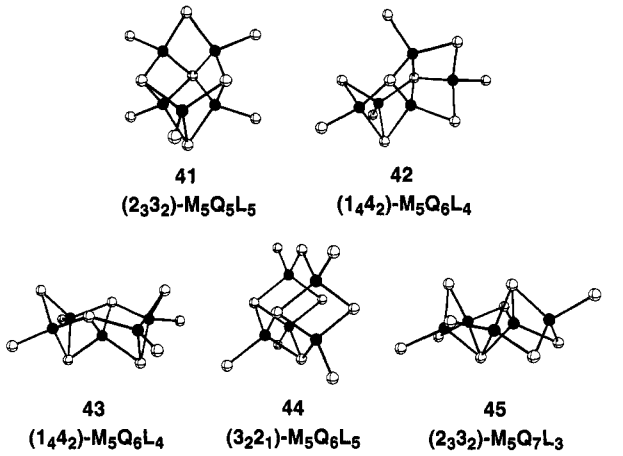

Figure 13. All of the new uniterminally ligated M_5 database clusters with Q atom bridging modalities of four or less.

In selecting clusters of interest, care should be taken not to enforce empirically determined restrictive criteria with absolute rigor. For instance, it is quite possible that stable Fe–Q clusters containing μ_n-Q atoms with $n > 4$ exist but have not yet been characterized. Figure 15 displays a selection of some of the more symmetrical and aesthetically pleasing structures that violate this bridging modality condition. All of these clusters are uniterminally ligated; however, each contains a single μ_5 (**58**), μ_6 (**59–61**), or μ_8 (**62**) Q atom. Cluster **58** corresponds to the lower half of the wrapped cluster **37**, from which it originated. The structures of **59** and **60** were derived from fragments, while **61** resulted from two folds. Cluster **62** is unique in that it represents the smallest antifluorite fragment and database cluster with no terminal ligands ($l = 0$). Precedence for this structural arrangement, including the μ_8-Q, is found in both $[Cu_8I_{13}]^{5-}$ and the core of $Cu_8S(S_2P(OC_2H_5)_2)_6$.[58,89] Structures **59**, **60**, and **62** are invertomers of **10**, **47**, and **14**, respectively.

Cluster Energetics

For a given chemical formula $M_mQ_qL_l$, what is the most energetically stable structure? This question can now be answered

(85) (a) Fenske, D.; Ohmer, J.; Hachgenei, J. *Angew. Chem., Int. Ed. Engl.* **1985**, *24*, 993. (b) Brennan, J. G.; Siegrist, T.; Stuczynski, S. M.; Steigerwald, M. L. *J. Am. Chem. Soc.* **1989**, *111*, 9240. (c) Fenske, D.; Krautscheid, H. *Angew. Chem., Int. Ed. Engl.* **1990**, *29*, 1452. (d) Krautscheid, H.; Fenske, D.; Baum, G.; Semmelmann, M. *Angew. Chem., Int. Ed. Engl.* **1993**, *32*, 1303.

(86) Adamson, G. W.; Bell, N. A.; Shearer, H. M. M. *Acta Crystallogr.* **1982**, *B38*, 462.

(87) As a corollary, basket-handle bridges are also the only means by which a tree can correspond to a uniterminally ligated cluster.

(88) The M_2Q_3 infinite double chain structure corresponding to the end member ($n = \infty$) in this series is present in $BaFe_2Q_3$ (Q = S, Se).[36]

(89) Rath, N. P.; Holt, E. M. *J. Chem. Soc., Chem. Commun.* **1985**, 665.

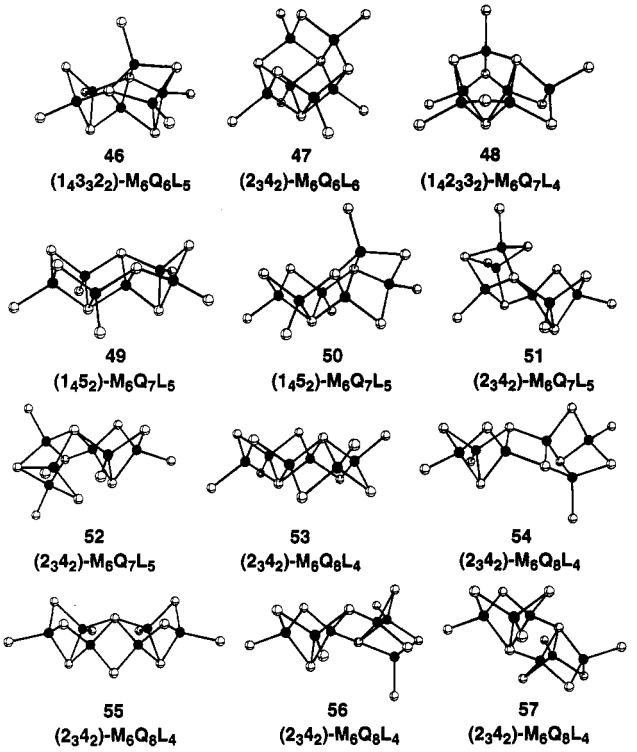

Figure 14. All of the new uniterminally ligated M_6 database clusters with Q atom bridging modalities of four or less.

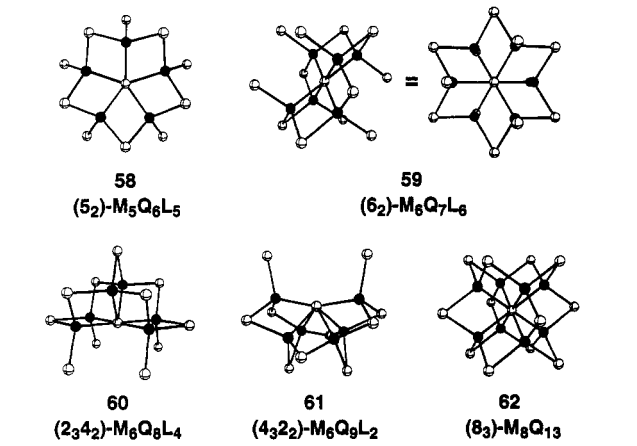

Figure 15. Selected uniterminally ligated database clusters containing a Q atom with bridging modality greater than four.

(at least within the context of the cluster database) by carrying out a series of electronic structure analyses based on calculations performed at whatever level of sophistication is deemed appropriate. In general, the cluster-generating techniques described here will lead to idealized structures containing regularly defined metal coordination geometries with standardized bond lengths. Thus, for simple qualitative comparisons, extended Hückel-type calculations[90] should prove sufficient. Furthermore, the speed and facility of this method is particularly conducive to the large number of calculations typically required. The overall approach to comparing cluster stabilities is demonstrated for iron–sulfur clusters selected from our database of structures composed of edge-sharing tetrahedra. All calculations employed the program CACAO[91] (PC version 3.0.1), with atomic parameters borrowed from other work.[92] To avoid any redetermination of L coordinates, chloride was chosen as a terminal ligand, leading to clusters of

(90) (a) Hoffmann, R.; Lipscomb, W. N. *J. Chem. Phys.* **1962**, *36*, 2179, 3489. (b) Hoffmann, R. *J. Chem. Phys.* **1963**, *39*, 1397.
(91) Mealli, C.; Proserpio, D. M. *J. Chem. Educ.* **1990**, *67*, 399.
(92) (a) Summerville, R. H.; Hoffmann, R. *J. Am. Chem. Soc.* **1976**, *98*, 7240. (b) Silvestre, J.; Hoffmann, R. *Inorg. Chem.* **1985**, *24*, 4108.

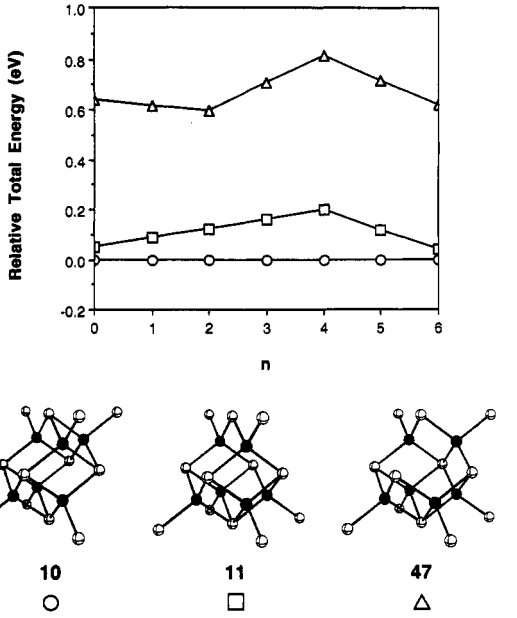

Figure 16. Relative total energies for the clusters $[Fe_6S_6Cl_6]^{n-}$ with structures **10** (prismane), **11** (basket), and **47**. Iron oxidation states vary with cluster charge, ranging from all ferric (n = 0, left) to all ferrous (n = 6, right).

formulae $[Fe_mS_qCl_l]^{n-}$. All Fe–S and Fe–Cl bond lengths were fixed at 2.26 Å.

As shown in Table 6, a chemical formula may give rise to more than one structural isomer, despite the imposed selection criteria. Consider, for example, clusters with formula $M_6Q_6L_6$. Of the nineteen different database structures, three (**10**, **11**, and **47**) fulfill the selection criteria, and are therefore of primary interest. A careful inspection of these three structures reveals them to be closely related. The difference between structures **10** (D_{3d}) and **11** (C_{2v}) lies in the position of one M atom and its associated terminal ligand. Similarly, **11** and **47** (C_{2v}) differ only in the position of one ML moiety. Alternatively, these structures may be viewed as the three isomers that result from pulling two ML moieties off of structure **14** in a reverse fusion-type process. In any case, the differences are so slight that it is difficult to construct an altogether convincing argument as to why one structure should be more stable than another. Consequently, to determine the relative stabilities of the three structures, we must calculate and compare their total energies. Figure 16 displays the results of these calculations for the clusters $[Fe_6S_6Cl_6]^{n-}$. The conclusions drawn are independent of cluster charge: structure **10** (prismane) is slightly more stable than **11** (basket), which is, in turn, considerably more stable than **47**. This trend is particularly satisfying on several counts. First and foremost, it is in agreement with experiment, which has shown that the clusters $[Fe_6S_6Cl_6]^{2-,3-}$ do indeed adopt the prismane structure.[45a,b] Second, the other known structure is only slightly higher in energy, and hence, it is reasonable for us to expect that a perturbation (such as replacing some or all of the chlorides with phosphines) might be enough to reverse the ordering. Finally, the unknown structure (**47**) is much less stable than either of the known structures, indicating a thermodynamic explanation for it not being observed. This thermodynamic instability must be inherent in the geometric arrangement of the structure, but it is not a simple consequence of any difference in bond lengths or local stereochemistries.

Table 7 summarizes the results of similar calculations for clusters with fewer than seven iron atoms. All formulae with more than one database structure meeting the selection criteria are included. The relative stability of clusters containing known iron–sulfur core geometries (**8**, **10**, **11**, and **12**) lends a certain degree of credibility to the results presented. However, there are a few points that should be kept in mind when examining this

Table 7. Relative Stabilities of Selected $[Fe_mS_qCl_l]^{n-}$ Clusters

formula	total energy ordering[a]
$[Fe_4S_4Cl_6]^{2-,3-}$	**23 ≈ 25 < 22 < 21 < 24**
$[Fe_4S_4Cl_6]^{(4-6)-}$	**22 < 23 ≈ 25 < 21 < 24**
$[Fe_4S_5Cl_4]^{(2-6)-}$	**32 < 33 < 26**[b]
$[Fe_5S_6Cl_4]^{(1-6)-}$	**42 < 43**
$[Fe_5S_6Cl_5]^{(2-7)-}$	**8 < 44 ≪ 58**
$[Fe_6S_6Cl_6]^{(0-6)-}$	**10 < 11 ≪ 47**
$[Fe_6S_7Cl_5]^{(1-7)-}$	**51 ≪ 49**[b] **< 50**[b] **≪ 52**
$[Fe_6S_8Cl_4]^{(2-4)-}$	**54 < 56 < 57 < 53**[c] **< 55 ≪ 60**
$[Fe_6S_8Cl_4]^{(5-8)-}$	**54 < 56 < 57 < 55 < 53**[c] **≪ 60**
$[Fe_6S_9Cl_2]^{(2-8)-}$	**12 ≪ 61**

[a] Symbols ≈ and ≪ indicate a total energy difference of less than 0.05 eV and greater than 0.5 eV, respectively. [b] Contains one fewer fold. [c] Contains two fewer folds.

table and associated structures. The total energy orderings displayed are specific to the iron–sulfur–chloride system and do not necessarily apply to the same structures for other chemical systems. Actual Fe–S bond lengths show some variation, depending on the bridging modality of the sulfur atom, and this is not factored into these idealized structures. The nature of the folding process is such that the metal centers involved are drawn closer together. In iron–sulfur clusters, any such crowding is alleviated by a distortion of the iron coordination away from an ideal tetrahedral geometry. This type of distortion has not been accounted for in any of our folded structures, which subsequently contain some Fe–Fe distances shorter than those present in unfolded structures. Thus, in the strictest sense, unambiguous comparisons can only be made between clusters containing the same number of folds. For $m \leq 4$, only two stoichiometries with multiple structures arise, and since uniterminal ligation does not hold for these smaller clusters, all of their isomers are compared in Table 7. Three structures (**58**, **60**, and **61**) included in Table 7 contain a sulfur atom with a bridging modality greater than four, in violation of the selection criteria. In all three cases, these structures are significantly higher in energy than isomers that meet the criteria, further supporting the use of Q atom bridging modalities in selecting stable structures.

Applications

Access to a complete structural database for a cluster family unleashes an enormous potential for application. Its most obvious utility is as an aid in cluster synthesis. Stable synthetic targets and byproducts can frequently be recognized, and results from energetic comparisons may sometimes lead to unexpected new synthetic pathways. Further, explicit structural information on possible or likely products is useful in many aspects of their characterization, including the interpretation of spectra and, ultimately, X-ray structure solution. Numerous other applications (often involving structure prediction for clusters that have not yet been, or cannot be, structurally elucidated) may depend on the particular cluster family. Some applications specific to our iron–chalcogenide cluster database are outlined next.

Ramifications of the structural database on iron–chalcogenide cluster synthesis and reaction chemistry should, for the most part, be readily apparent in many of the preceding sections. Based on selection criteria and energetic comparisons detailed above, the following clusters (structures) appear to be viable new synthetic targets: $Fe_4Q_5L_4$ (**26**), $Fe_5Q_5L_5$ (**41**), $Fe_5Q_6L_4$ (**42**), $Fe_5Q_7L_3$ (**45**), $Fe_6Q_5L_6$ (**9**), $Fe_6Q_6L_5$ (**46**), $Fe_6Q_7L_4$ (**48**), $Fe_6Q_7L_5$ (**49**), $Fe_6Q_7L_5$ (**51**), $Fe_6Q_8L_4$ (**53**), and $Fe_6Q_8L_4$ (**54**). Total energy comparisons such as the one plotted in Figure 16 sometimes exhibit crossings, implying that the most stable structure is dependent upon the metal oxidation state. If one of these structures is adopted by a known cluster, then simple redox chemistry may provide a route to the other structure. For example, calculations comparing $2[Fe_3S_4(PH_3)_3]^{n-}$ (**5**) and $[Fe_6S_8(PH_3)_6]^{2n-}$ (**40**) predict that at lower iron oxidation states ($n \geq 0$) the former structure is considerably more stable than the latter. Thus, reduction (or attempts at synthesis under more reducing conditions) of the cluster $[Fe_6S_8(PEt_3)_6]^+$ may cleave it in a process reversing the condensation shown in Figure 12, providing a widely sought route to clusters with structure **5**.

Iron–sulfur clusters are present in many important proteins and enzymes, in whose chemistry they frequently play a pivotal role.[93] To achieve a complete understanding of how these biomolecules function, it is necessary that we first obtain an accurate structural assessment of them, including their iron–sulfur cluster components. This is most reliably accomplished through a detailed crystallographic study. Sometimes the structural resolution obtained with current X-ray techniques may not be sufficient for direct structure determination of the comparatively small metal clusters. In such cases, a typical recourse is to propose a model for the cluster structure and then determine how well it fits the observed electron density. The model with the best fit is refined and accepted as the correct structure. A problem inherent in this method is the distinct danger of overlooking reasonable (and possibly correct) structures when proposing and testing models. Clearly, this is a situation in which access to a complete database of plausible cluster structures would be of obvious value. Through the use of experimentally confirmed features (at the very least, the approximate number of iron and sulfur atoms) associated with the cluster under investigation, all reasonable structures could be extracted from the database, and subsequently tested. As the protein environment has been shown to stabilize unprecedented structures,[82] none of these possibilities should be excluded on the basis of structural precedent or energetic comparisons. Such a process should significantly reduce the likelihood of a catastrophic error (an incorrect structure) and increase confidence in the final results. Appropriate database subsets for iron–sulfur clusters in biomolecules which have not yet been fully structured may be found elsewhere.[94]

Recently, there has been a growing interest in cluster ions produced by laser ablation, a technique in which a solid sample is directly pulsed with the beam of a laser. The chemical composition of cluster ions formed under such conditions can then be determined by mass spectrometry. Iron–sulfur cluster anions produced by laser ablation of samples containing various ratios of iron and sulfur have been characterized in such a fashion, and a considerable amount of speculation has been devoted to their structures.[95] Photodissociation studies performed on the cluster ions indicate a possible relationship between their structues and the core geometries found in known iron–sulfur clusters.[95b] If this relationship holds, then our database could provide an exhaustive source of candidates for cluster ion structures. Figure 17 displays a selection of proposed structures for observed iron–sulfur cluster anions. These structures were derived by simply removing all terminal ligands, leaving a naked Fe_mS_q cluster core. Whenever possible, selection was based on the hypothesis that a structure containing all three-coordinate iron atoms (i.e. cores deriving from uniterminally ligated clusters) is more stable than one containing some two-coordinate irons. Similarly, preference was given to structures fulfilling the S atom bridging modality criteria. It seems probable that these structures might undergo some rearrangement, due to the absence of saturating terminal ligands. Certain molecular mechanics packages may be capable of modeling such rearrangements, using the structures in Figure 17 as starting geometries. The cluster ions produced in the laser ablation of numerous other binary metal–oxide/chalcogenide systems have been characterized, and construction of structural

(93) Cammack, R., Ed. *Adv. Inorg. Chem.* **1992**, *38*. This volume contains a collection of articles on Fe–S clusters in biology.
(94) Long, J. R.; Holm, R. H. *Inorg. Chim. Acta*, in press.
(95) (a) El Nakat, J.; Fisher, K. J.; Dance, I. G.; Willet, G. D. *Inorg. Chem.* **1993**, *32*, 1931. (b) Yu, Z.; Zhang, N.; Wu, X.; Gao, Z.; Zhu, Q.; Kong, F. *J. Chem. Phys.* **1993**, *99*, 1765.

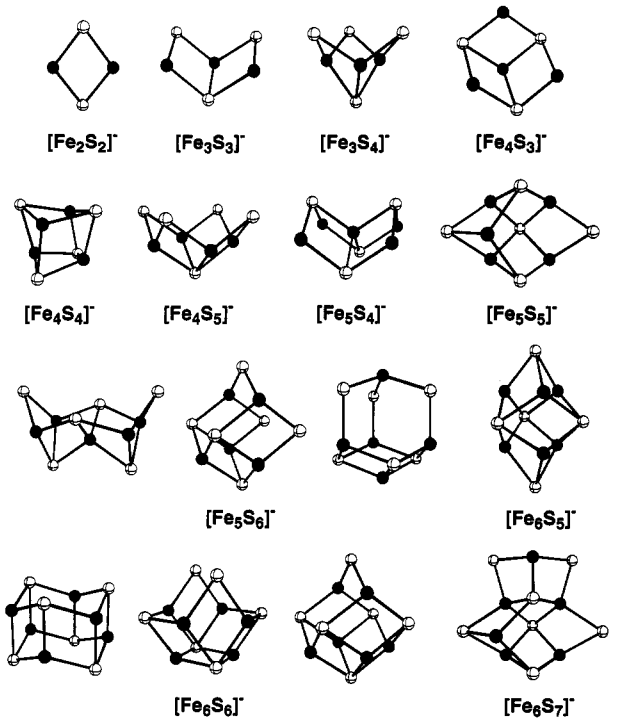

Figure 17. Proposed structures for observed laser ablated iron–sulfur cluster anions containing six or fewer iron atoms.

databases specific to these systems should proceed along the guidelines described herein.

Appendix: Polyhedra Connectivity Partitioning (PCP) Notation

Countless painstakingly drawn structures showing not atoms, but polyhedra are testimony to the importance of their connectivity in the description of large clusters[76,96] and extended solids.[76,97] Such pictures often fail in their attempt to convey the three-dimensional information obtainable through handling a physical model. As the complexity of the structure grows, the amount of useful information retrievable from a two-dimensional drawing dwindles. In actuality, the chances of extracting a false piece of information also increase, rendering a carelessly drawn figure detrimental. A notation analogous to that introduced above for graphs may be used to accurately summarize the polyhedra connectivities, eliminating any possible confusion associated with a figure. For certain applications, the descriptor itself may be sufficient, conserving the often considerable effort involved in creating a picture. More importantly, the development of such a notation marks the first step toward a general theory of polyhedra-based structures.

Clusters. Consider a structurally resolved cluster with chemical formula $M_mQ_qL_l$ containing m metal centers (M), q anionic bridging atoms (Q), and l unidentate terminal ligands (L). Given that each metal center displays a recognizable polyhedral coordination environment, the polyhedra may be partitioned by degree of connectivity for use as a structural descriptor by applying the following set of general rules.

(1) Assign an appropriate symbol (P) for the polyhedron corresponding to the ligand environment of each metal center, as listed in Table 8. List the polyhedral types present in order of decreasing coordination number (CN) and v(max) (i.e., moving from the bottom to the top in Table 8), and consider each in turn.

(96) Pope, M. T. *Heteropoly and Isopoly Oxometalates*; Springer-Verlag: Berlin, 1983.

(97) (a) Wells, A. F. *Structural Inorganic Chemistry*, 5th ed.; Oxford University Press: Oxford, 1984. (b) Hyde, B. G.; Andersson, S. *Inorganic Crystal Structures*; John Wiley & Sons: New York, 1989.

Table 8. Descriptive Symbol and the Maximum Vertex-Sharing Number for Some Common Polyhedral Coordination Environments

CN	polyhedron	symbol	v(max)
2	linear	L	1
3	trigonal planar	Δ	2
4	square planar	S	2
	tetrahedron	T	3
5	trigonal bipyramid	ΔB	3
	square pyramid	SPy	4
6	octahedron	O	3
	trigonal prism	ΔP	4
8	cube	C	4
	square antiprism	SA	4
12	icosahedron	I	3
	cuboctahedron	CO	4
	anticuboctahedron	ACO	4

$$PP'P''... \tag{7}$$

(2) Let the *vertex-sharing number*, v, be defined as the number of vertices one polyhedron shares with another. In other words, v is the number of Q atoms connecting one metal center to another by M–Q bonds. Thus, for a tetrahedral center, v = 1, 2, and 3 corresponds to corner, edge, and face sharing with another polyhedron. The vertex-sharing number for two metal centers may take on any integral value from 0 to v(max), where v(max) is the maximum number of vertices that can be shared due to the obvious spatial constraints (see Table 8). Determine all of the different non-zero vertex-sharing numbers that arise from a polyhedral center of a given type, and list them in order of descending subscript, v.

$$P_{v(\max)}...P_2P_1 \tag{8}$$

(3) Consider each vertex-sharing situation (P_v) in turn. As described above for points in graphs, partition the polyhedra by degree of connectivity, $P_v(...n_i...)$, where n is the number of polyhedra with symbol P that share exactly v vertices with each of exactly i other polyhedra. In other words, n is the number of metal centers that are connected by v Q atoms to i different metal centers through M–Q bonds. Since the cluster contains m metal centers, n and i must have upper bounds of m and $m-1$, respectively (i.e., since there are a total of m polyhedra, no more than m of them can have a specific connectivity, and any one of them cannot be connected to more than $m-1$ others). List these partitions in order of decreasing i.

$$P_v(n_{m-1}...n_2n_1) \tag{9}$$

(4) Append the chemical formula to yield the full descriptor in PCP notation.

$$P_{v(\max)}(n_{m-1}...n_1)...P_1(n_{m-1}...n_1)P'_{v'(\max)}(n_{m-1}...n_1)...\\ P'_1(n_{m-1}...n_1)...\text{–}M_mQ_qL_l \tag{10}$$

While this general formulation appears unwieldy, it is almost always the case that the symmetrical structures preferred by nature contain only a few different polyhedra, resulting in relatively compact descriptors. Further, depending on the context in which the notation is employed, it is often possible to use only the most relevant portions of the full descriptor, yielding a reduced descriptor. Such is the case for the edge-sharing tetrahedral structures described above.

(5) For heterometallic clusters, a PCP descriptor is evaluated for each different type of metal as described in steps 1–4 above. The descriptors are then listed in the order in which their corresponding metals appear in the chemical formula and separated by vertical lines.

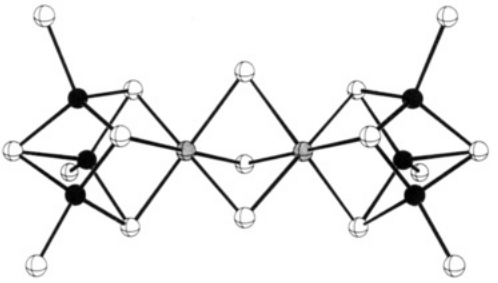

Figure 18. The structure of $[V_2Fe_6S_8(SEt)_9]^{3-}$. Gray, black, and white spheres represent V, Fe, and S atoms, respectively. Ethyl groups (not shown for clarity) are bonded to the six terminally ligated and the three doubly bridging S atoms.

$$...P_v(n_{m-1}...n_1)...|...P'_{v'}(n_{m'-1}...n_1)...|...P''_{v''}(n_{m''-1}...n_1)... -M_mM'_{m'}M''_{m''}...Q_qL_l \quad (11)$$

The full process of deriving the PCP notation for a heterometallic cluster is detailed next.

The cluster $[V_2Fe_6S_8(SEt)_9]^{3-}$ takes on the double cubane structure shown in Figure 18.[98] We will now derive its PCP descriptor by following the above rules for both metals simultaneously. Both V atoms display octahedral coordination, and all Fe atoms are tetrahedrally coordinated.

$$O|T \quad (12)$$

The V octahedra exhibit edge sharing ($v = 2$) and face sharing ($v = 3$), while the Fe tetrahedra share only edges.

$$O_3O_2|T_2 \quad (13)$$

The two V octahedra share a single face ($n = 2$ for $v = 3$ and $i = 1$) with each other and three edges ($n = 2$ for $v = 2$ and $i = 3$) with Fe tetrahedra. Each of the six Fe tetrahedra share exactly three edges ($n = 6$ for $v = 2$ and $i = 3$), two with other Fe and one with a V.

$$O_3(2_1)O_2(2_3)|T_2(6_3) \quad (14)$$

Finally, by appending the chemical formula, we arrive at the full descriptor.

$$O_3(2_1)O_2(2_3)|T_2(6_3)-[V_2Fe_6S_8(SEt)_9]^{3-} \quad (15)$$

Given this descriptor a chemist may, with a little bit of thought, arrange two octahedra and six tetrahedra into the double cubane structure. As mentioned above for graphs, a descriptor is not necessarily unique. On occasion, more than one possible structure may be recognized. Further examples of the PCP notation are given in Table 2, which also introduces a reduced notation for edge-sharing tetrahedral structues.

Solids. The above treatment of polyhedral clusters lends itself easily for application to infinite solid systems. Only two slight modifications are necessary, and the notation for some common structures is demonstrated in Table 3.

(1) Clearly the partitioning must be defined differently for an extended solid, since the number of polyhedra in a crystal is, for all practical purposes, infinite (a number that is notoriously difficult to partition). Thus, we shall redefine n as the number of crystallographically distinct metal centers that are connected by v Q atoms to i different metal centers through M–Q bonds. Two atoms are *crystallographically distinct* if their atomic coordinates are not related by the symmetry of the crystal.

(2) To distinguish the notation from that used for clusters, the chemical formula may be prefixed by a subscript ∞ and a superscript d, where d is the number of dimensions in which the structure is infinitely extended (i.e., $d = 1$, 2, or 3).

$$..._{\infty}^{d}M_mQ_qL_l \quad (16)$$

This dimensionality prefix was first introduced by Machatschki,[99] and it is in keeping with the current "crystal chemical formula" notation.[100]

Acknowledgment. This work was supported by NIH Grant No. GM 28856. We thank Dr. D. M. Proserpio for supplying a copy of CACAO and Prof. I. G. Dance for a helpful discussion.

Supplementary Material Available: Tables enumerating formulae for $M_7Q_qL_l$ and $M_8Q_qL_l$ clusters composed of edge-sharing tetrahedra (4 pages). This material is contained in many libraries on microfiche, immediately follows this article in the microfilm version of the journal, and can be ordered from the ACS; see any current masthead page for ordering information.

(98) Cen, W.; Lee, S. C.; Li, J.; MacDonnell, F. M.; Holm, R. H. *J. Am. Chem. Soc.* **1993**, *115*, 9515.

(99) Machatschki, F. *Naturwissenschaften* **1938**, *26*, 67, 87.

(100) Lima-de-Faria, J.; Hellner, E.; Liebau, F.; Makovicky, E.; Parthé, E. *Acta Crystallogr.* **1990**, *A46*, 1.